DOE/PC/88921--8

DE92 004498

DOE Technical Report No. DOE/PC/88921-8
Eighth Quarterly (Second Annual) Report on Research Grant No. DE-FG22-88PC88921
Title: SPIN-MAPPING OF COAL STRUCTURES WITH ESE AND ENDOR
Principal Investigators: R. L. Belford and R. B. Clarkson
Institution: University of Illinois at Urbana-Champaign
Date: September 1, 1990

US/DOE Patent Clearance is not required prior to publication of this document.

Because this is not only a quarterly but also an annual report, a cumulative summary of highlights is submitted. During this quarter, the Office of Program Analysis in the Department of Energy has required the Principal Investigators to prepare a comprehensive report in preparation for an oral presentation for a peer review of projects in the Fossil Energy Advanced Research programs. The appropriate sections of this comprehensive report therefore serves as the 8th quarterly/2d annual report for DE-FG22-88PC88921:

Sections 1.-4.: These sections, pp. 1-8 of the Office of Program Analysis report, are omitted because they contain only file information concerning project personnel, funding from other sources, professional biographies, information of collaborators, and the like. The present report therefore starts with Section 5.

5. PROJECT OVERVIEW

A. Specific Project Objectives

A nondestructive method to determine the atomic and molecular structures present in the organic (maceral) components of whole coal and coal products has been sought for many years. This program of research is designed to address that analytical need by applying advanced electron magnetic resonance techniques to the determination of coal molecular structure. Structural information has be obtained by using the naturally occurring unpaired electrons in coal as "observation posts" from which to survey neighboring atoms through the electron-nuclear hyperfine interaction. Such an overall approach has been termed **ELECTRON SPIN MAPPING** of coal structure. New techniques like 2-dimensional ENDOR and ESE spectroscopies and multifrequency EPR, including the world's first S-band ESE spectrometer and one of the first W-band instruments, which we have developed in our laboratory, were employed in the determination. The materials studied were well separated macerals obtained by density gradient centrifugation techniques from Illinois #6 coals, a well as whole Illinois #6, #5, and Argonne Premium Sample Coals. Model compounds, chosen to represent molecular structures typical of those believed to exist in coal also were studied by the various electron magnetic resonance (EMR) methods.

Utilizing the various EMR methods available in our laboratory, we studied approaches to determine parameters that **directly reflect** the atomic and molecular structure of coal. The naturally occurring unpaired electrons in coal were utilized as probes of their local environment, which they reflect through hyperfine interactions with neighboring $I > 0$ nuclei (eg, ^{1}H, ^{13}C).

Specifically, work has focussed on the following areas:

1. **Measurement of hyperfine interactions from ^{1}H and ^{13}C in well-separated macerals, whole coals, and model compounds.**

Experiments on macerals and coal rely primarily on ESE, although 2-Dimensional ENDOR also has been employed. Work on coal model compounds has involved both ESE and ENDOR.

2. **Measurement of very high frequency spectra of coal and separated macerals.**

A W-band (96 GHz) EPR spectrometer has been constructed, and applied to the study of coal with good results. In particular, the spectra show excellent sensitivity to heteroatoms (e.g. O, S), and may be useful in studying organic aromatic sulfur in coal.

3. **Data Analysis**

Several aspects of data analysis have been developed, including the use of simplex algorithm to optimize the fit between ESE, ENDOR, and EPR data and theoretical simulations. Significant work also has been performed on the theory of ESE data, particularly ESEEM results.

4. **Oxygen Effects**

In the course of preparing samples for study by EMR techniques, we observed a strong effect on the signal of oxygen partial pressure. This interaction is particularly strong in fusinite macerals. We have studied the nature of oxygen interactions on fusinite, and have developed an EPR method to measure oxygen partial pressures in situ that utilizes this effect.

5. **MRI Imaging of solvent penetration in coal**

In the course of preparing solvent extracts of coals for this study, we became aware of the need to characterize in greater detail the coal/solvent interactions, and therefore developed a method to study solvent penetration by magnetic resonance imaging (MRI).

B. This work relates to the DOE mission to develop better methods to characterize fossil fuels, in order to better utilize these energy resources.

C. This project is designed to develop new electron magnetic resonance methods for coal characterization, and thus is complementary to other projects in the areas of physical characterization, magnetic resonance, and coal analysis.

D. Project History

We have been working for almost seven years to understand the relationships that exist between powder EMR spectra and the structure of materials. Much of this work has focussed on coal and coal model systems. The following grants have partially supported this work.

PROJECT TITLE	DURATION	FUNDING SOURCE	DIRECT COSTS	INDIRECT COSTS
EPR and ENDOR Studies of Changes in Coal from Desulfurization	9/82-8/83	IDENR/CRSC	$40,000	$4,500
Electron Spin Mapping of Coal Molecular Structure by ENDOR	9/84-8/87	DOE/PETC (University Coal Reserach)	125,808	48,934
Mapping Coal Structure with ESE Spectroscopy	9/85-8/86	IDENR/CRSC	66,000	10,000
Studying Coal Molecular Structure with ESE	9/86-8/87	IDENR/CRSC	70,000	12,000
ENDOR and ESE Studies of Radicals formed on Metal Oxide Surfaces	9/87-9/89	PRF/ACS	34,000	1,000
Spin Mapping of Coal Structures with ESE and ENDOR	9/88-8/91	DOE/PETC (University Coal Reserach)	141,984	72,700
EPR Microscopy of High-Sulfur Illinois Coals	9/88-8/90	IDENR/CRSC	152,050	15,205
VHF EPR Determination of the Chemical Forms of Organic Sulfur in Coal	9/90-8/91	IDENR/CRSC	74,350	14,870

IDENR/CRSC is the Illinois Department of Energy and Natural Resources, which funds the Center for Research on Sulfur in Coal.

6. SCIENTIFIC AND TECHNICAL CONTENT

A. Schedule of major research activities

9/88 Inception of grant.

11/88 First ^{13}C ESEEM from coal.
S-band Pulsed EPR spectrometer first is used to study coal.

3/89 Orientation selection seen in ENDOR of thianthrene(+).

9/89 Simplex optimization is implemented.

10/89 ENDOR parameters for coronene(+) and perylene(+) are optimized.

11/89 W-band EPR of coals and separated macerals is accomplished.
W-band spectra of model compounds (perylene, dibenzothiophene, dibenzofuran).

12/89 FID from evacuated coal identified as originating from fusinite.
Oxygen effects on EPR signals from fusinite are observed.
W-band spectra of the Argonne Sample Bank Coals are obtained.

2/90 MRI of solvents in coal is first accomplished.

3/90 Theory of orientation effect in powder ENDOR is developed.

5/90 Theory of orientation effects in ESEEM is developed.

6/90 Q-band ENDOR instrument is demonstrated.
Hypothesis for lineshapes in W-band spectra of coal is stated.

9/90 Swelling parameters are evaluated for DMSO in Illinois #5 and #6 by MRI.

B. Scientific issues being addressed, experimental approaches taken, and importance of problem.

A major objective in coal science continues to be the nondestructive determination of atomic and molecular structure in the individual components that comprise this heterogeneous mineral. Work on questions seemingly as different as the geologic origin of different macerals and the effects of various coal cleaning technologies would benefit greatly from detailed atomic information about coal structure. **Because of its heterogeneous and complex nature, the microscopic structure of coal will not be entirely understood through the use of a single physical method, and it is not productive to view research in this area as a contest between various techniques.** Rather, several different approaches should be used in a complementary way, each contributing part of the information that is needed to develop a more comprehensive and useful map of coal atomic and molecular structure.

Since nondestructive techniques are all relatively new, most of what we know about the composition of coal comes from destructive methods. Attempts to deduce the native structure of coal from mass spectral, NMR, separation science, and infrared data on components derived from chemically or thermally treated samples have led to the development of two main approaches for the modeling of maceral structure -- parameters and average molecular construction. Parameters include such average structural information as aliphatic/aromatic carbon ratios and number of aromatic rings per molecule. Average molecular construction approaches attempt to devise a solid maceral structure that will account for the molecular structures found in products. Several examples of this second method are given in the following references [1, 2, 3, 4, 5]. Figure 1 illustrates one of these structures, that developed by Shinn for an average bituminous coal maceral [3].

The importance of coal models (and detailed information on microscopic structure) is growing as work on more complex processing methods seeks to relate **coal properties** with **coal molecular and atomic structure**. Because of the many uncertainties in relating composition data obtained from destructive analytical methods to the native structures in coal, there is a need both for nondestructive approaches to the determination

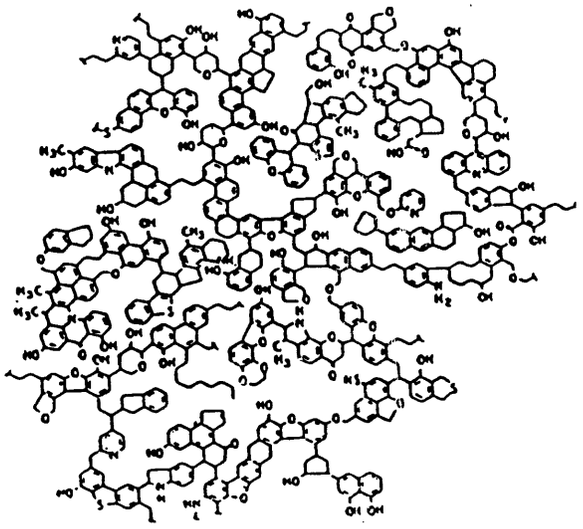

Figure 1. Shinn's model of bituminous coal structure [3].

of atomic and molecular structure and for information about specific coal samples rather than statistical information on average properties. Among the relatively few nondestructive methods capable of observing coal structure on this microscopic scale, magnetic resonance methods (EPR, NMR, ENDOR, ESE) are showing great promise. This is because these methods have, in many cases, developed theoretical and experimental ways to achieve the 1) sensitivity, and, 2) resolution needed to determine microscopic structure in non-crystalline, opaque, and relatively non-volatile solids like coal.

Among magnetic resonance spectroscopies, none is more sensitive than Electron Paramagnetic Resonance (EPR). It was natural that two of the first studies ever undertaken with the then-new technique (ca. 1953) were investigations of the unpaired electrons naturally occurring in coal [6, 7]. From the very beginning of EPR work on coal, it was apparent that the technique had enormous sensitivity, but that by itself it lacked sufficient resolution to observe the very small hyperfine splittings that contain information on the atomic and molecular structure "observed" by the electron. Although NMR usually has the ability to resolve much smaller splittings, it
also was unable to achieve the necessary resolution to determine coal molecular structure directly, and was hampered by sensitivity problems as well. One potential solution to these difficulties emerged with the advent of Electron-Nuclear Double Resonance (ENDOR) spectroscopy, a hybrid technique that can be characterized as NMR with detection by EPR (e.g. NMR resolution with EPR sensitivity), and which is specifically designed to resolve hyperfine interactions.

In 1981, Retcofsky and co-workers reported the first successful resolution of electron-nuclear hyperfine interactions (other than matrix effects) in several Pennsylvania whole coals using ENDOR [8]. They saw hyperfine couplings characteristic of those expected in aromatic hydrocarbons, as well as one coupling possibly from an aliphatic moiety. The similarity of couplings from several coals generally supported the view that macerals may be composed of a limited number of functional groups, linked together in varying combinations and concentrations. Such information is exactly the sort needed to develop specific information on the molecular structure of coal, and demonstrated the potential of the technique. The overall approach of using unpaired electrons in coal to

observe atomic and molecular structure was termed **HYPERFINE FINGERPRINT SPECTROSCOPY.**

For the past five years, our laboratory has worked on extensions of the ENDOR technique as applied to the structural determination of coal. We have developed computer-controlled instrumentation capable of performing complex ENDOR experiments involving **two variables**, which we term 2-dimensional ENDOR, and which have shown tremendous promise in increasing still further the spectral resolution of the technique for coal work. We also have developed theoretical methods for analyzing the powder ENDOR spectra obtained from coal samples, and have performed many experiments on model systems as well. We are developing a library of ENDOR spectra from powders containing model compounds (eg, anthracene, naphthalene, pyrene, perylene, dibenzothiophene, etc), which we will use to begin the analysis of data from whole coals [9]. In addition, we have built a time-domain (pulsed) EPR spectrometer optimized for coal studies, and have begun to employ it to do Electron Spin Echo (ESE) spectroscopy with excellent results [10].

The importance in coal research of **nondestructive** analytical methods cannot be overemphasized. Not only do these methods get information about truly unmodified coal, they allow accurate comparisons to be made between raw coal and material that has been treated by various cleaning technologies, thus providing benchmark data on the effects of cleaning as well as on the native coal. Some questions cannot be answered by any other approach -- questions concerning the distribution of organic sulfur compounds along micropores in coal being a case in point.

Among nondestructive methods, magnetic resonance techniques represent some of the very few capable of getting information about both chemical composition and compound location. We believe that the electron magnetic resonance approaches developed by us over the last five years (with partial support from the CRSC and the U.S. DOE) offer a unique analytical view of organic sulfur in coal. **Specifically, and with reference to the six goals given above, we believe that this program is making significant contributions to our understanding of organic sulfur in coal in the following ways:**

1. **Chemical characterization:** nondestructive determination of the molecular structures of sulfur-containing organic compounds in both whole coal and in separated macerals. This is a goal of enormous importance. Applications of such information to the analysis of coal, as well as to the design, optimization, and evaluation of coal cleaning technologies are too numerous to list. By obtaining hyperfine fingerprint spectra from whole coal and separated macerals, our electron magnetic resonance technique can measure components of this structure, and **by the sulfur g-shifts, fingerprints associated with sulfur compounds can be identified.**

2. **Physical characterization:** obtaining precise data (± 0.1Å) on the interatomic distances, number density, and arrangement of atoms in individual macerals. This, to be accomplished by high-resolution pulsed EPR microscopy, will help us to understand the influence of sulfur on the physical characteristics of coal, processed coal, and separated macerals. The advent of excellent methods of maceral separation (eg density gradient centrifugation) has focussed attention on the large differences in organic sulfur content of various maceral components. **Details of the physical differences between different maceral types will improve understanding of these sulfur concentration differences, and will help to suggest optimal strategies for sulfur removal.** The information also will be important in assessing the effects of various coal cleaning technologies. Our electron magnetic resonance method

can nondestructively provide this information with a precision unrivaled by other techniques.

3. **Physical characterization:** micron-resolution spatial imaging of coal samples. In recent years, magnetic resonance imaging has made dramatic advances in image clarity, resolution, and chemical information content. Our laboratory has developed unique instrumentation to do electron magnetic resonance imaging microscopy, which we propose to use to study the distribution of sulfur-containing species and maceral domains in whole coal and separated materials. **Obvious areas of importance to coal science include: 1) the nondestructive mapping of sulfur compounds in different macerals and at various boundaries such as pores and inorganic mineral inclusions in whole coal, 2) analysis in space and time of solvent penetration into the coal matrix. Modern digital image reconstruction techniques allow us to develop images (maps) of only sulfur compounds, or of other, more general organic chemical species with a resolution of 1 micron (or better).**
4. **Physical and chemical characterization:** obtaining hyperfine fingerprint data from selected volume elements in a piece of whole coal. This is another important and complementary capability of imaging technology. Our goal here is to get chemical structure information on sulfur compounds in individual macerals without the necessity of physically separating the components. Such a nondestructive "magnetic resonance dissection" is possible because of the tremendous sensitivity of our electron magnetic resonance spectroscopy. **Such a capability would be very useful in the routine analysis of coal, as well as in evaluating the effects of coal cleaning on different portions of the coal, without actually destroying the samples and introducing uncertainties into results.**

We have made substantial progress implementing and using these new experimental methods to non-destructively characterize coals.

Because this program is based on several different magnetic resonance techniques, a detailed description of each method will not be given here. Instead, the basic physical principles underlying the procedures will be described in enough detail to explain the experiments, results, and conclusions that follow in subsequent sections.

1) VHF W-Band EPR

The fundamental motivation for building a spectrometer to perform the EPR experiment at a magnetic field of 3.4 T. instead of at the usual 0.34 T. is to improve spectral resolution and sensitivity of the technique to sulfur-containing compounds. The relationship between magnetic field strength and sensitivity to sulfur can be better understood by considering the energy of an unpaired electron in an external field, **B**. If the atomic or molecular orbital of the electron is nondegenerate (L = 0), then the "spin only" energy is given by:

$$\mathcal{H}_{ez} = \beta_e \mathbf{B} \cdot \mathbf{g} \cdot \mathbf{S}, \qquad \text{(i)}$$

where $\mathcal{H}_{ez}$ is the spin Hamiltonian (electronic Zeeman interaction only), β_e is the Bohr magneton, **B** is the external magnetic field, **g** is the g-tensor, and **S** is the electron spin operator. In this case, when the electron possesses only spin angular momentum, the g-tensor is isotropic and has the free electron value $g_e = 2.00232$.

When the electron is in an orbital with angular momentum (L > 0), either by itself

or via coupling to excited states, then the orbital angular momentum mixes with the spin angular momentum. Our Zeeman spin Hamiltonian now contains another term, reflecting this additional interaction:

$$\mathcal{H}_{ez} = \beta_e \mathbf{B} \cdot \mathbf{L} + g_e \beta_e \mathbf{B} \cdot \mathbf{S}, \text{ or}$$

$$= \beta_e \mathbf{B} \cdot (\mathbf{L} + g_e \mathbf{S}). \quad \text{(ii)}$$

In addition to modifying the electronic Zeeman energy, the orbital angular momentum of the unpaired electron (or the magnetic dipole moment induced by the orbital motion) also interacts directly with the unpaired electron, creating an additional energy term:

$$\mathcal{H}_{so} = \lambda \mathbf{L} \cdot \mathbf{S}, \quad \text{(iii)}$$

where λ is the spin-orbit coupling constant, a term proportional to the nuclear charge of the atom (Z) and $1/r_3$, where r is the orbital radius. λ may be positive or negative, reflecting the fact that the local orbital field may add to or subtract from the external static field.

The total spin energy for this system now is written:

$$\mathcal{H}_{SPIN} = \mathcal{H}_{ez} + \mathcal{H}_{so} = \beta_e \mathbf{B} \cdot (\mathbf{L} + g_e \mathbf{S}) + \lambda \mathbf{L} \cdot \mathbf{S}. \quad \text{(iv)}$$

The effect of orbital angular momentum is to alter the energy of the spin in an external magnetic field. We now must remember that in the EPR experiment, we measure the energy represented by $\mathcal{H}_{SPIN}$, not by scanning frequency, but by scanning magnetic field. Field positions of resonance lines are related to energies by the simple resonance equation:

$$h\nu = g_{eff} \beta_e B_o,$$

where all symbols have their customary meaning, and g_{eff} is an "effective g-value" that characterizes the position of the line (analogous to the chemical shift parameter in NMR). If L = 0, then $g_{eff} = g_e$, as can be seen in Equ. (iv); if L > 0, then g_{eff} will deviate from g_e in a way determined by L and λ. In the coal system, spin-orbit coupling ($\mathcal{H}_{so}$) is primarily responsible for this deviation, and this key fact allows us to observe the presence of organic sulfur compounds in the EPR spectra.

2) Pulsed S-band EPR and ESE

Although the ideas behind ESE techniques are as old as magnetic resonance itself (1946), the general application of spin echo methods to paramagnetic systems has occurred in only the last few years with the advent of very high speed digital electronics under computer control. Unlike the familiar continuous wave (cw) EPR experiment, which has been available in commercial instrumentation for nearly 20 years, ESE spectroscopy is not yet a commercially available technique, and only a dozen or so laboratories throughout the world currently perform the experiment. For an excellent review of the theory and early applications of ESE spectroscopy, the book by Kevan and Schwartz is recommended [11].

Unlike cw EPR, ESE is a pulsed microwave experiment. Very short microwave pulses excite the paramagnetic spin system, and the time evolution of the magnetization is monitored. Certain pulse schemes, characterized by the number of degrees the

magnetization vector is tipped by each pulse, are known to generate a strong instantaneous magnetization in the sample following the sequence. Typical pulse schemes known to induce this rephasing or "echo" effect are 90^{o}-T-180^{o} (Hahn echo sequence) and the 90^{o}-t-90^{o}-T-90^{o} (stimulated echo sequence). We have found the stimulated echo sequence, diagrammed in Figure 2, to be most useful in our coal studies.

ESE spectroscopy has many advantages over the more conventional cw EPR. Chief among the advantages for our coal work is that, like ENDOR, the technique may be used to obtain spectra which resolve hyperfine structure that is obscured in cw spectra by inhomogeneous line broadening. In order to understand how ESE can be made to accomplish this task, let us look at the characteristics of the information obtained in the experiment.

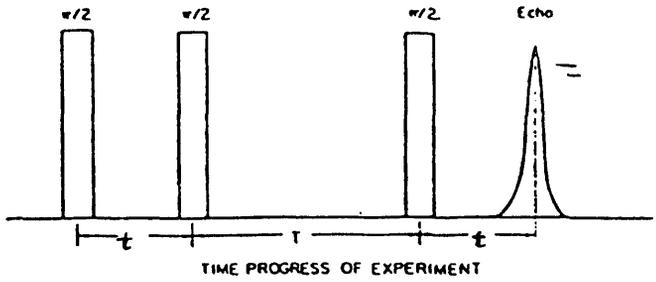

Figure 2. Timing diagram of stimulated-echo pulse sequence. Typical pulse ~40nsec; times t and T range from .001 to 1 msec.

In a typical stimulated echo experiment done on coal, the time interval t between the first and second 90^{o} pulse is set at a fixed value during the experiment, while the interval T between the second and third pulses is incremented in steps, as shown in Figure 3. The amplitude of the echo induced by the sequence is measured as a function of the delay time T between the second and third pulses. In the absence of any interactions between the unpaired electrons being observed and neighboring nuclei with non-zero magnetic moments, the variation of the echo amplitude V with the delay time T is given by the simple exponential function:

$$V_{echo}(2t + T) = V_{o} \exp [(2t + T)/T_{m}], \qquad (v)$$

where Tm is the phase memory time of the individual spin packets. The exponential decay curve describing the echo amplitude as a function of T is called the electron spin echo envelope.

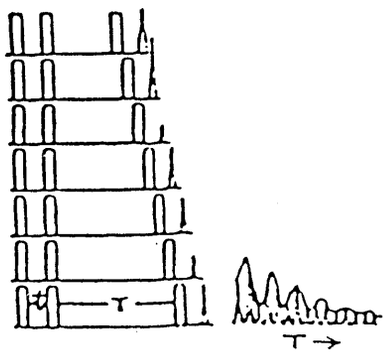

Figure 3. Measurement by the method of stimulated echoes, showing ESEEM.

If our unpaired spins experience hyperfine interactions with neighboring nuclei, these interactions will manifest themselves as modulation patterns in the ESE envelope. This phenomenon is thus known as electron spin echo envelope modulation (ESEEM). For an S= 1/2, I= 1/2 system with isotropic g-values (a very good approximation in the case of coal) and two hyperfine interactions characterized by frequencies f_a and f_b, the ESEEM pattern (without echo decay) is given by:

$$V_{mod}(2t+T) = 1 - k\{\sin^2(f_a t/2)\sin^2[f_b(t+T)/2] + \sin^2(f_b t/2)\sin^2[f_a(t+T)/2]\} \quad \text{(vi)}$$

In this expression, k is the so-called modulation depth parameter, proportional to B_o^{-2} in the limit of small hyperfine interactions (B_o being the value of the static external magnetic field). For more than one nucleus, V_{mod} is the product of the modulation functions of the individual nuclei:

$$V_{mod} = V_{mod}(I_1)\cdot V_{mod}(I_2)\cdot V_{mod}(I_3)\cdot \ldots \quad \text{(vii)}$$

Thus, for the case of n like nuclei coupled identically to an electron spin, the overall modulation is given by the modulation function for one nucleus raised to the n^{th} power. The overall modulated signal in the time-domain spectrum is then the product of these two functions:

$$V_{echo}(2t + T) = V_{decay} \cdot V_{mod} \quad \text{(viii)}$$

A Fourier transform of the ESEEM pattern results in a frequency domain spectrum exhibiting linewidths that are characteristic of individual spin packets rather than of the entire envelope of spin packets comprising the inhomogeneously broadened lines observed by cw EPR. Since the modulation frequencies can be analyzed by an ENDOR-like theory, this technique provides us with a powerful alternative way of resolving the hyperfine interaction energies normally obscured in the cw spectra of whole coal. This information, in turn, allows us to study the environment experienced by radicals in coal, as well as giving us information on the structure of the radicals themselves. ESE and ENDOR thus provide two complementary routes to the study of coal molecular and atomic structure.

Finally, we can simulate the time-domain ESEEM pattern described in Equ. (vii) on the basis of coal structural models involving distances between the unpaired electron and nuclei with non-zero magnetic moments, numbers of atoms, and orientations. By fitting theoretical simulations to experimental data, detailed atomic structural information is obtained.

3) Magnetic Resonance Imaging

Three dimensional EPR imaging has been developed in the Illinois ESR Research Center to achieve precise nondestructive microscopic spatial resolution of internal structures in opaque objects. Good reviews of the method can be found in References 12, 13, and 14. The symmetry constraints placed on samples by two dimensional methods are completely removed in this implementation.

Spatially resolved data are obtained with a set of rectangular transverse field

gradient coils, mounted on circular z-gradient coils, and rotated about the z axis to produce any desired gradient. The field gradients act as scales to measure distances or positions, and the raw data comes encoded in terms of magnetic fields. Through sophisticated computer back reconstruction algorithms, this field-encoded data is used to construct three dimensional pictures of the object, including high-resolution microscopic images of internal structures. The software controlling data acquisition currently can obtain images of a small object in a series of 200 micron "slices" of arbitrary orientation (the orientation can be decided on after the experiment is finished and the data is being processed).

It also is possible to image protons using NMR imaging techniques. We have worked to develop two and three-dimensional imaging techniques utilizing the protons in various solvents as the reporting spins. This work has been in collaboration with the staff of the Biomedical Magnetic Resonance Laboratory, Prof. Paul Lauterbur, director, and the staff of the National Center for Supercomputing Applications (NCSA, NSF) and the Beckmann Institute. Solvent penetration and swelling studies have been performed on various Illinois coals, including Illinois #6 (Herrin County) and Illinois #5 (Galatin County). Water, methyl alcohol, acetone, and DMSO have been thus far used as solvents. Instrumentation for the studies is located in the BMRL, and consists of a SISCO imager with a 4.7 Tesla 30 cm bore magnet, and various RF and field gradient coils optimized to give the best signal-to-noise and spatial resolution. Currently we are using a probe/gradient system built by Doty, Inc., Fort Collins, CO.

7. PROJECT OUTPUT

A. Major recent accomplishments

1. Multi-frequency EPR of Coal

Multi-frequency EMR is the method of making electron magnetic resonance measurements (e.g. EPR, ENDOR, ESE) on the same material at several, substantially different, microwave frequencies, in order to obtain more complete and precise information relating the magnetic and chemical/structural properties of a system. Previous applications of the approach to EPR spectroscopy of coal have demonstrated its effectiveness, even over a modest two-frequency range (9.5 GHz and 35 GHz) [15,16], and the entire subject recently has been reviewed by Belford and co-workers [17], who point out that multi-frequency studies of complex systems often can facilitate reliable interpretations of structure, bonding, and magnetic interactions that would otherwise remain uncertain or impossible to analyze in single-frequency experiments. These authors demonstrate that an examination of the principal terms of the spin Hamiltonian provide a useful starting point for understanding the utility of multi-frequency experiments.

Let the spin Hamiltonian, $\mathcal{H}_s$, be written as the sum of electronic and nuclear spin operators,

$$\mathcal{H}_s = \mathcal{H}_e + \mathcal{H}_n, \tag{1}$$

in which

$$\mathcal{H}_e = +|\mu_B|\mathbf{B}_o \cdot \mathbf{g}_e \cdot \mathbf{S}, \qquad S = \tfrac{1}{2}, \tag{2}$$

and

$$\mathcal{H}_n = -g_n|\mu_n|\mathbf{B}_o \cdot \mathbf{I} + \mathbf{S} \cdot \mathbf{A} \cdot \mathbf{I}, \qquad I = \tfrac{1}{2}; \tag{3}$$

$\mathbf{B}_o$ denotes the external magnetic field while $\mathbf{A}$ represents the hyperfine interaction matrix. The first term in each part of $\mathcal{H}_s$ describes the Zeeman interaction (electronic or nuclear), and is characterized by a dependence on $\mathbf{B}_o$ and expressions containing g-values. The

second term in $\mathcal{H}_n$ describes the hyperfine interactions between electrons and nuclei.

Information on structure and bonding is contained in both the Zeeman and hyperfine interactions, which together form the basis for an experimentally observed electron magnetic resonance spectrum. Because of the complexity frequently seen in spectra from disordered, heterogeneous systems like coal, it can be very difficult to analyze or unambiguously interpret the data. For example, the EPR linewidths of coal spectra can include contributions from g-anisotropy and hyperfine interactions, and it usually is difficult to determine the relative importance of each contribution. In this case, one would like to "switch off" the hyperfine interaction for one observation, and then compare the resulting spectrum with a conventional one containing both Zeeman and hyperfine terms in order to separate the two contributions. Magic-angle spinning attempts to do just this, for example, by averaging away the dipolar portion of I_1,I_2 interactions in NMR spectroscopy, and other NMR techniques address different portions of $\mathcal{H}_s$ to effect spectral simplifications. Unfortunately, the much more rapid electronic relaxation rates exhibited by paramagnetic systems have thus far made it impossible to apply these techniques to EMR. What is needed for EMR is a method to vary the importance of terms in the spin Hamiltonian that does not depend critically on relaxation rates -- a goal which the multi-frequency approach accomplishes. By performing EPR, ENDOR, or ESE at different microwave frequencies (and hence in different B_0 ranges), it is possible to emphasize or de-emphasize Zeeman interactions relative to hyperfine terms, allowing a more critical evaluation of many spectral effects, among which are the following: g-dispersion (EPR) [18]; nuclear Larmor frequencies, orientation selection (ENDOR) [19]; echo envelope modulation depth [20], orientation selection [21, 22], exact cancellation [23] (ESE); relaxation rates (seen in all methods). For example, Figure 3 shows EPR spectra of an Illinois #6 coal taken at three different frequencies. As g-dispersion increases with B_0, the appearance of a low-field shoulder becomes obvious. In this instance, important chemical information contained in the electronic Zeeman term could be revealed only at higher frequencies.

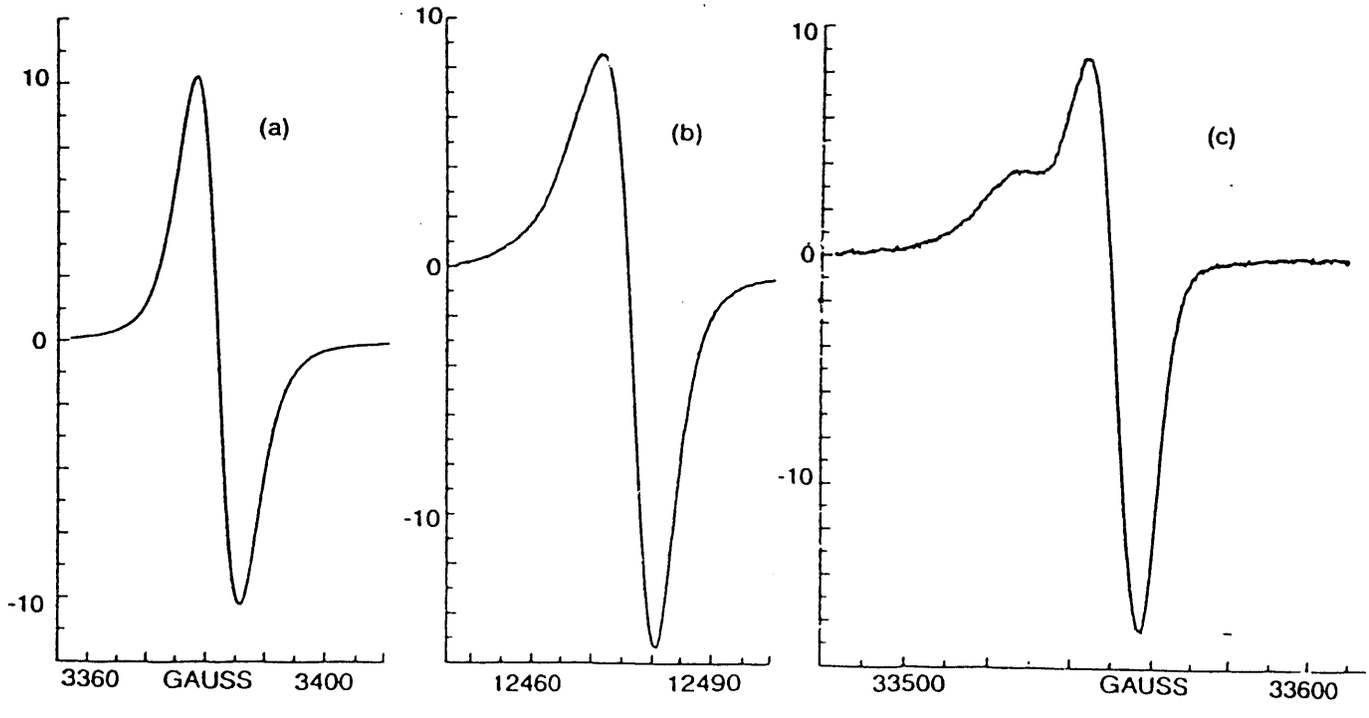

Figure 3. EPR spectra of an Illinois #6 coal. (a) 9.5 GHz, (b) 35 GHz, (c) 95 GHz.

In this portion of the report, we describe very high frequency (96 and 250 GHz) EPR work on coals from the Argonne Premium Coal Sample (APCS) program and the Illinois Basin Coal Sample Program (IBCSP). Other related ongoing work in our laboratory includes multi-frequency ENDOR and ESE studies of coal.

EXPERIMENTAL

Samples of coal from the Argonne Premium Coal Sample Program were received in sealed glass ampoules under nitrogen. The compositions of these eight samples have been reported [24]. For EPR at 96 GHz (VHF EPR), the ampoules were opened in air just prior to taking spectra. Samples were loaded into 0.5mm I.D. capillaries and placed in the cavity of the spectrometer. The W-band (96 GHz) instrument has been described elsewhere[4]. Field strengths were measured with an NMR gaussmeter (Metrolab model 2025); frequencies, with a digital frequency counter (EIP model 578) A variety of sharp, solution phase samples were used to insure precise g-calibration.

A sample of Illinois #6 coal from the Illinois Basin Coal Sample Program (IBCSP #1) was separated by density gradient centrifugation prior to study, and vitrinite, sporinite, and fusinite maceral fractions were analyzed prior to taking EPR spectra. The analysis data for these samples is given in Table I.

Table I. Elemental and Proximate Data for IBCSP #1
Dry Ash Free Basis

Sample	Dry %C	Dry %H	Dry %N	Dry %S	Dry %O
1822 whole	76.9	4.9	1.3	3.3	13.7
Vitrinite	75.7	5.3	1.4	2.6	11.6
Sporinite	76.2	5.9	1.1	3.9	12.9
Fusinite	79.6	4.2	1.3	2.0	12.8

The maceral composition of the IBCSP #1 coal was determined to be 87% vitrinite, 4.4% liptinite, and 8.6% inertinite. The separated vitrinite from this coal was also studied on a 250 GHz spectrometer built by Freed et. al. at Cornell University [25].

Model compounds (perylene, dibenzothiophene, and dibenzofuran) were prepared as cation radicals either by adsorbing the materials as gasses onto an activated silica-alumina catalyst (Houdry M-46) [26], or by UV irradiating boric acid glasses containing the compounds in 10 - 50 mM concentrations.

Samples for ESE study were evacuated for 24 hours at room temperature and pressures $< 10^{-4}$ Torr in 5mm thin-walled NMR tubes. They then were sealed in the glass. The S-band (2-4 GHz) ESE spectrometer used in the study has been described previously[6].

RESULTS AND DISCUSSION

1) VHF EPR

Figures 4(a-h) show room temperature W-band spectra of all eight coals from the

Argonne Premium Coal Sample Program. The samples show a considerable range of line shapes, in some cases revealing features not seen at lower field strengths. Because of our special interest in high-sulfur Illinois coals, we have begun the analysis of these spectra with APCS #3 (an Illinois #6). Many of the points that have thus far been considered in this analysis should find application in the interpretation of the VHF EPR spectra of other coals.

The most prominent features of the W-band spectrum of APCS #3, in addition to the largest peak, include a low-field shoulder and a broad, weak, high-field wing. In order to determine whether these features are characteristic of a particular maceral, W-band spectra were taken of vitrinite, sporinite, and fusinite components separated from an analogous Illinois #6 (IBCSP #1) by the density gradient centrifugation method. Spectra of the three separated macerals are shown in Figures 5(a-c). These spectra clearly show substantial spectral variation with maceral type, and we will consider each in turn.

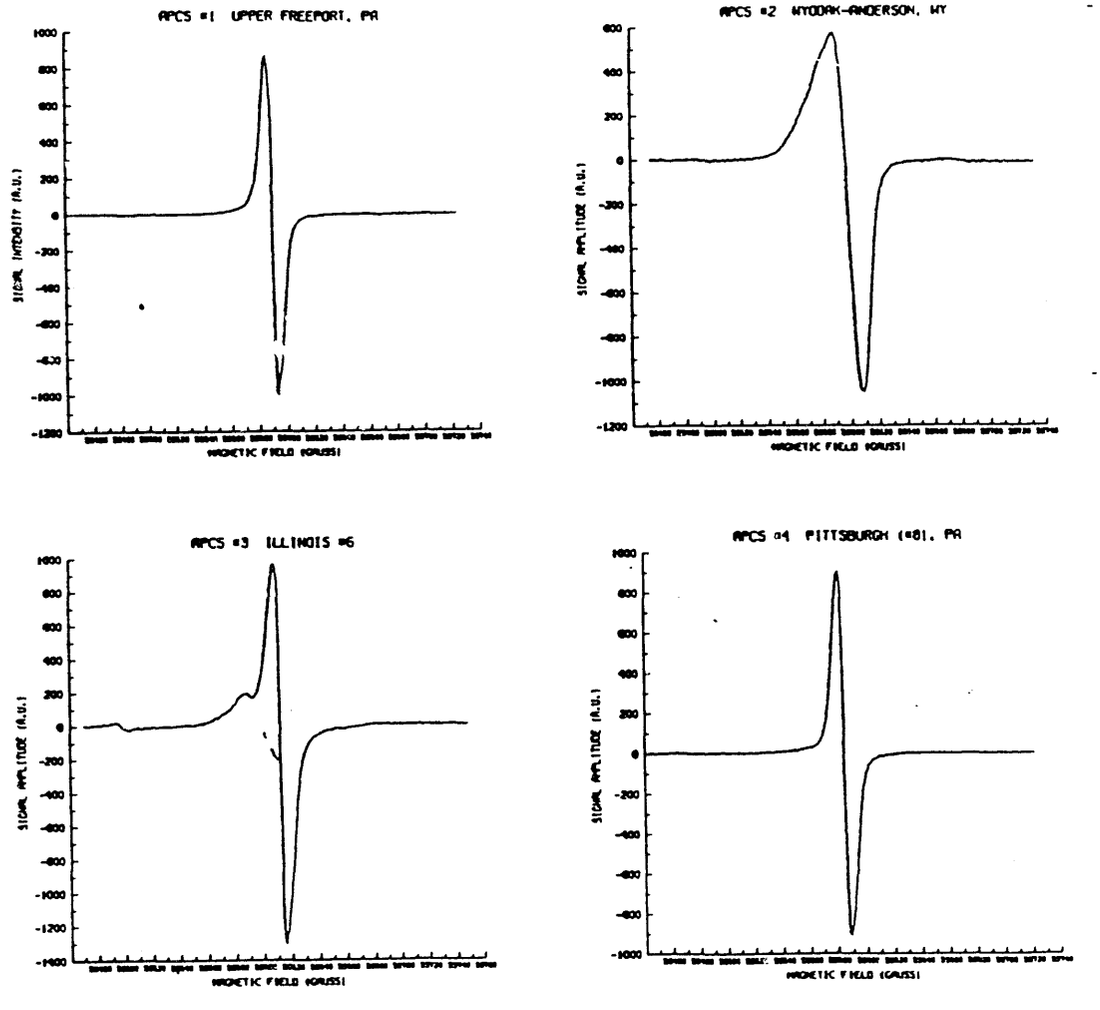

Figure 4. W-band EPR of Argonne Premium Coal Samples.

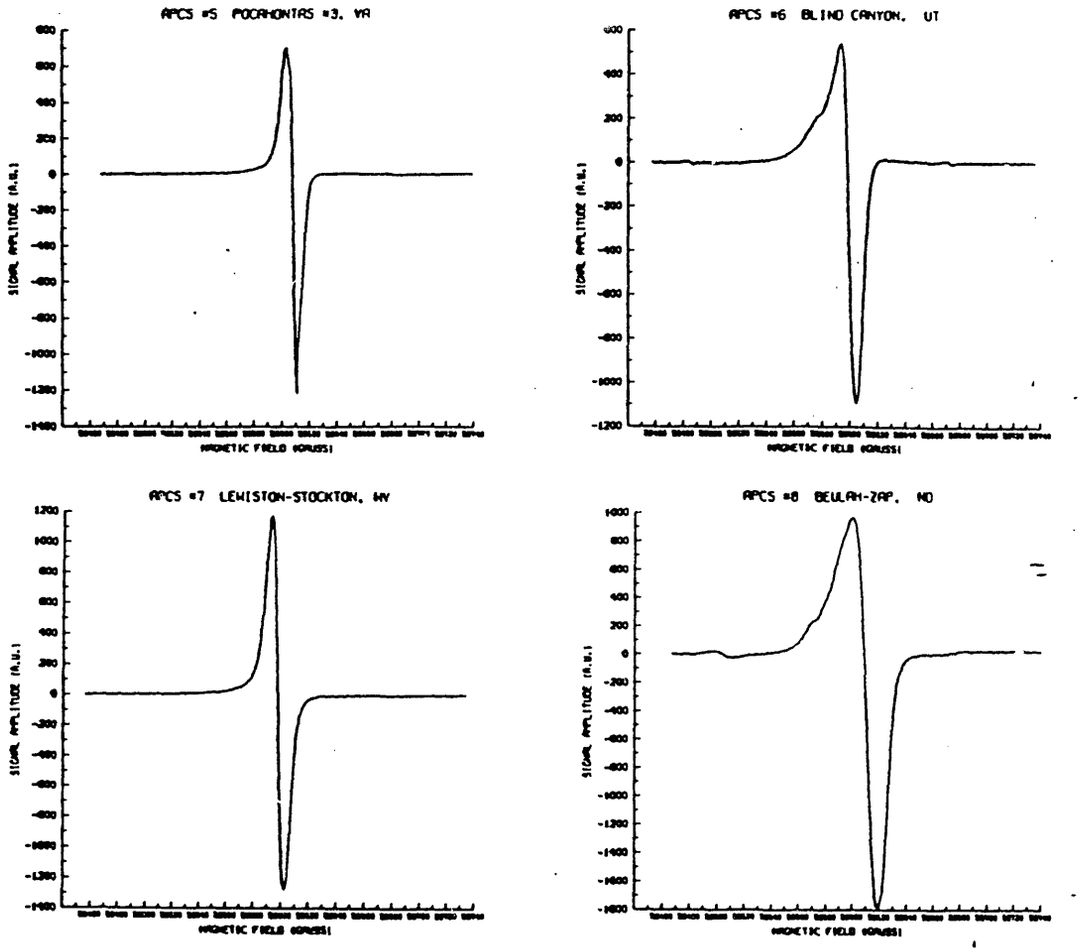

Figure 4. (con't). W-band EPR of Argonne Premium Coal Samples.

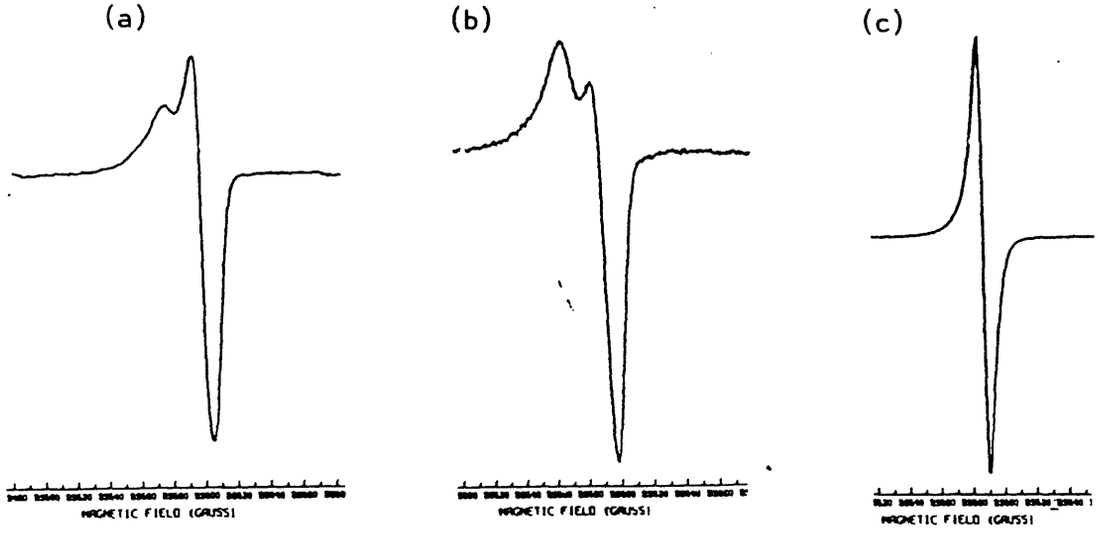

Figure 5. W-band of (a) vitrinite, (b) sporinite, and (c) fusinite from an Illinois #6.

The fusinite signal in Figure 5(c) is so different from the other two maceral spectra, it must reflect a dominant interaction that is not as important in the other components. This interaction usually is assumed to be electron spin exchange, resulting in a narrowing of the resonance line [15, 27]. We have tested this hypothesis by performing S-band pulsed EPR measurements on the fusinite, and observe only a free induction decay (FID), as shown in Figure 6. A very strong dependence of T_1e and T_2e on adsorbed oxygen was observed in these measurements, and the fusinite sample whose FID is shown in Figure 6. was carefully evacuated. The observation of an FID, combined with the absence of echoes, lends strong

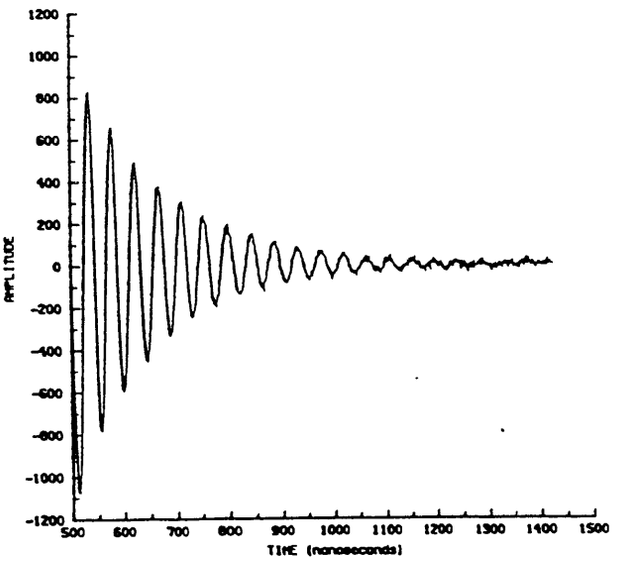

Figure 6. FID at S-band observed in the fusinite from an Illinois #6 using a single $\pi/2$ observing pulse.

support for the spin exchange model, particularly since the maceral contains almost as much hydrogen (4.24%) as the vitrinite and sporinite, which give strong spin echoes and proton ESEEM. Fourier transformation of the FID yields a frequency domain spectrum with linewidth nearly identical to that observed in the sample by CW EPR at 3, 9, and 96 GHz, again in agreement with the prediction of a linewidth independent of B_o for exchange narrowing in the limit $B_e >> B_o$ or $B_e << B_o$, where B_e is exchange field.

The simplest assumption would be to assume that the vitrinite spectrum in Figure 5(a) is due to a single paramagnetic species and to simulate it with an anisotropic g-matrix and suitable linewidth/line shape parameters. This has been done, and the result is shown in Figure 7, for $g_1 = 2.0023$, $g_2 = 2.00274$, and $g_3 = 2.0042$. However, chemical and spectroscopic evidence strongly suggests that this EPR spectrum is the result of contributions from two or more radical species with different heteroatom compositions. Thus, this simulation may be useful for identifying the approximate anisotropic g-values, but the fact that it accounts for the gross features of the spectrum should not be viewed as implying that the single species model is correct. As we shall see, more detailed comparisons of separated macerals, particularly vitrinite and sporinite from this sample, strongly suggest the presence of more than one paramagnetic species.

In order to confirm that the low-field peak in this spectrum is a part of an anisotropic lineshape (as opposed to a partially resolved symmetric peak), the separated vitrinite was run at 250 GHz in the laboratory of Professor Jack Freed (Cornell University). Figure 8

shows a comparison of the 96 and 250 GHz spectra and confirms that the low-field peak is, indeed asymmetric and part of one or more overlapping anisotropic spectra.

Comparison of vitrinite and sporinite spectra (Figs. 5(a) and (b)) begin to illustrate the difficulties of the simple model, since features with identical g-values appear with different

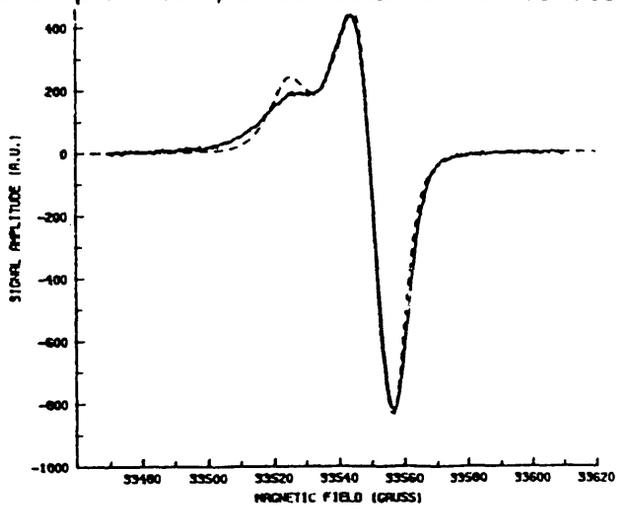

Figure 7. W-band spectrum of separated vitrinite: _____(experimental); (----)theoretical.

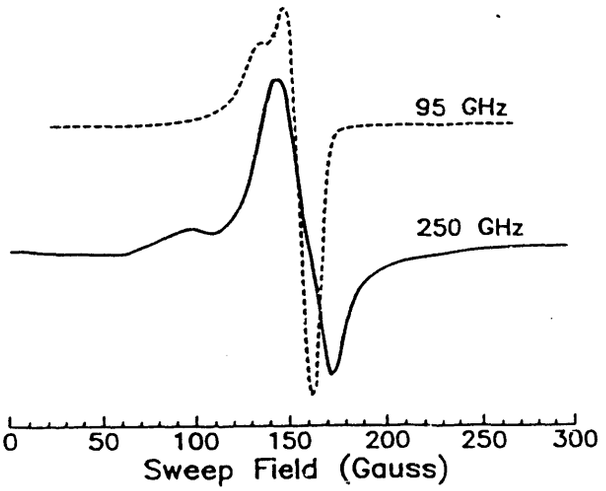

Figure 8. 95 and 250 GHz EPR spectra of a vitrinite separated from Illinois #6.

intensities in the two systems, suggesting the unequal contribution of two or more spectral components. The lower two g-values (g_1 and g_2) of the vitrinite are, in fact, just those observed for many different conjugated aromatic radicals, and predicted theoretically by Stone [28], and it is tempting to see the spectrum as a composite formed from pure hydrocarbon and heteroatomic radical contributions. In all probability, the low-field shoulder in this spectrum is associated with heteroatomic radicals, since spin-orbit (SO) coupling to sulfur (or oxygen) is the most likely mechanism to account for the higher value of g_3. The rather poor low-field fit of the single species simulation then could be a reflection of this composite character. Clearly, this issue of spectral and sample heterogeneity is of utmost importance for the correct interpretation of EPR spectra of fossil fuels, even when well-separated and purified, and we presently are working on several

approaches designed to shed more light on the problem.

Deviations of g factors (g-shifts) from the free-electron value (2.0023) and direction-dependence in g factors (g-anisotropies) result from admixture of orbital angular momentum (and therefore magnetic moment) into the spin angular momentum to augment (or diminish) the spin-only Zeeman splitting. An unpaired electron in an orbital Φ which includes some p, d, or f character on atom A is subjected to a spin-orbit coupling interaction characteristic of that particular atomic orbital; that interaction mixes excited-state spin orbitals into the ground-state spin orbitals $\Phi\alpha$ and $\Phi\beta$. As a rule, organic radicals which contain sulfur atoms display particularly strong g-shifts and g-anisotropies for the following reasons. Generally, 2p oxygen-atom orbitals are much more effective at spin-orbit coupling than carbon-atom orbitals, and 3p (or 3p,3d hybrid) sulfur-atom orbitals are a great deal more effective than oxygen. Moreover, sulfur heteroatoms in an aromatic pi-system radical tend to trap the electron spin density more than oxygen heteroatoms, thus enhancing the intrinsic relative effectiveness of sulfur atoms in causing g shifts. The g-anisotropies arise because the excited-state orbitals which are mixed into the ground-state semi-occupied molecular orbital) have directional properties. Finally, g-shifts may be positive or negative depending on the type of excited state which spin-orbit coupling mixes into the ground state; $\chi^2\Phi^1 \rightarrow \chi^1\Phi^2$ and $\chi^0\Phi^1 \rightarrow \chi^1\Phi^0$ transitions cause g-shifts of opposite sign.

One promising avenue of investigation involves comparing W-band EPR spectra from coal with spectra obtained from model compounds believed to typify organic structures in coal. Figure 9(a) shows a spectrum from perylene cation radicals, together with a preliminary theoretical simulation. The simulation used g_1 = 2.0024, g_2 = 2.0030, and g_3 = 2.0032, proton hyperfine values obtained experimentally by ENDOR[12], and spin packet linewidths determined by electron spin echo measurements. Figure 9(b) shows the

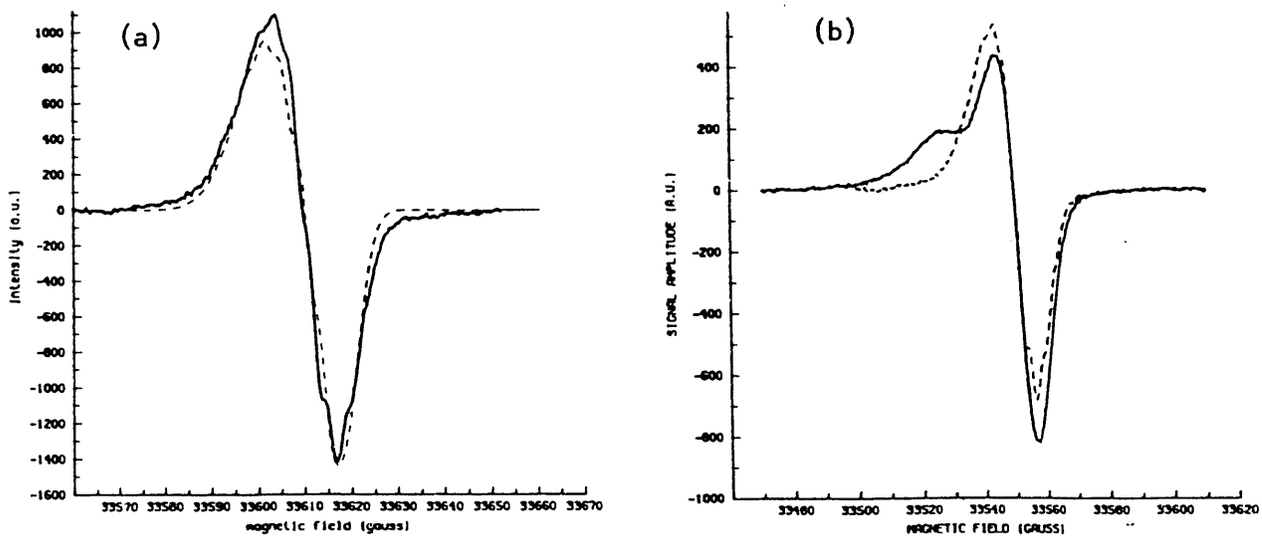

Figure 9. (a) W-band spectrum (_____) of perylene(+) and theoretical simulation (----); (b) superposition of vitrinite (_____) and perylene(+) spectra.

perylene(+) spectrum superimposed on a vitrinite W-band spectrum, to illustrate how a portion of the coal resonance line shape might originate from conjugated aromatic hydrocarbon radicals containing no heteroatoms.

Figure 10(a) shows a W-band spectrum of dibenzothiophene cation radicals,

together with a preliminary theoretical simulation (g_1 = 2.0016, g_2 = 2.0054, g_3 = 2.0106). The effect of SO coupling with sulfur is seen in the higher g-values and much more asymmetric line shapes. Attar and Dupuis reported that thiophenes are the most abundant form of organic sulfur in Illinois coals (thiophenic, 58%; Ar-S-Ar, 20%; R-S-R, 18%; Ar-SH, 15%; R-SH, 7%); thus this model compound should give us an indication of the sulfur-related effects that are to be expected [29].

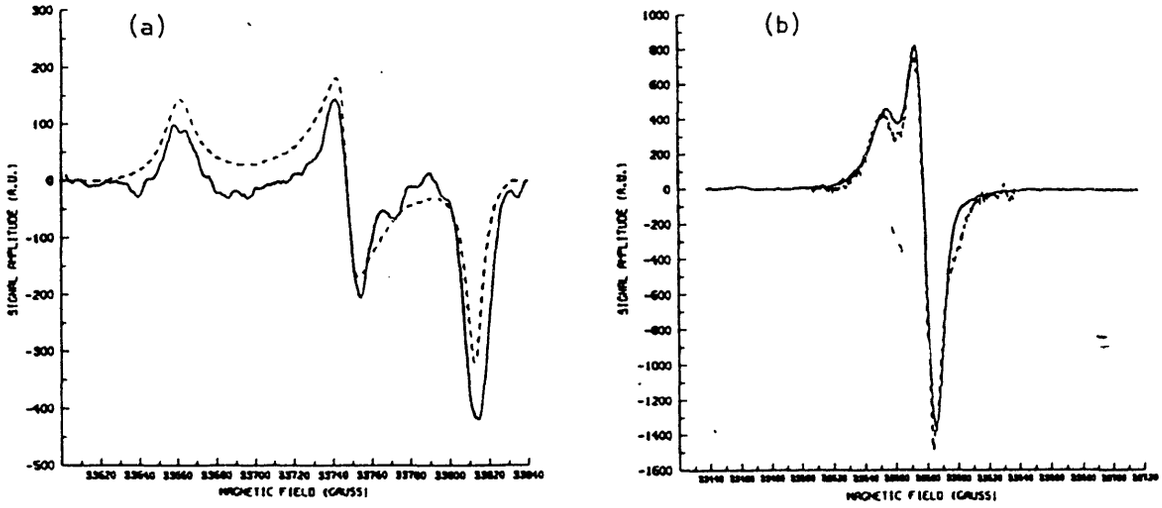

Figure 10. (a) W-band spectrum (_____) of dibenzothiophene(+) and theoretical simulation (----); (b) vitrinite (_____) and composite spectrum of perylene(+) and dibenzothiophene(+) (----).

Because conjugated aromatics are the predominant structural types for organic sulfur in this coal, and because unpaired electrons are expected to be most abundant (and stable) in such chemical environments, it seems likely that EPR spectra from coal will strongly reflect the delocalization of electrons. This implies that a very small number of sulfur (or oxygen) atoms can exert a large effect on spectral line shapes, making this technique uniquely sensitive to heteroatoms with larger SO coupling constants (λ). Since the effect of a sulfur atom on g-values decreases as an electron is delocalized over a larger and larger number of carbon atoms (and the S/C ratio falls), the precise line shapes from sulfur in coal will depend on the size of the aromatic structures, as well as on the type of bonding. This fact represents another opportunity for the nondestructive analysis of high-sulfur coals by W-band EPR, since it may be possible to model the spectra in order to get more detailed chemical information about the forms of organic sulfur that are present. To illustrate this concept, Fig. 10(b) shows a W-band spectrum of vitrinite. Superimposed on it is a composite spectrum constructed by adding the spectrum from perylene(+) and a portion of that from dibenzothiophene(+). While the agreement between data and construct is not perfect, a comparison does suggest that molecular forms like perylene and dibenzothiophene are contributing to the experimental spectrum, although it is very likely that neither of these species, as isolated structures, is a major component in coal. In the future, we hope to use spectral addition methods in a more quantitative way to gain a better understanding of the molecular structure of the organic components of coal, including organic sulfur.

2) ENDOR in coal model compounds

The first ENDOR and ESE results on whole coal were reported by Kevan and colleagues [30], focussing on proton matrix ENDOR effects. Retcofsky, et. al. published

ENDOR spectra from several Pennsylvania coals, resolving hyperfine interactions between unpaired electrons and protons bonded to the radicals [31]. These spectra held out the promise of identifying the radical species in coal based on the hyperfine couplings. Two principal points complicated interpretation: 1) ENDOR spectra from whole coals are the result of contributions from several different radical species, and, 2)ENDOR spectra from radicals in disordered solids exhibit significant hyperfine anisotropy, requiring the full theoretical simulation of spectra in order to arrive at an accurate interpretation. Because these two points each represent a complex problem in spectral interpretation, we decided to approach them separately, by using model compounds thought to exist as radicals in coal.

We adopted a technique whereby cation radicals of conjugated aromatic molecules are formed on the surface of activated silica-alumina and alumina powders. Samples prepared in this way have many of the spectroscopic characteristics of the radicals in coal. Because the ENDOR spectra of radicals in coal represent a "powder-like" pattern, and because there is considerable hyperfine anisotropy in conjugated aromatic radicals, it is impossible to obtain the principal elements of the hyperfine coupling tensors by simple inspection of the experimental results. A computer simulation of the results needs to be made, and a best fit of experimental and calculated spectra sought. This best fit then defines the A_x, A_y, and A_z values for each interaction. Our original ENDOR spectral simulations followed closely the approach used by Dalton and Kwiram [32], who simulated ENDOR using perturbation theory. A more rigorous simulation approach on which we now are working diagonalizes the spin Hamiltonian matrix rather than using perturbation theory expressions. The inclusion of g-anisotropy and quadrupole interactions also makes this new calculation more comprehensive. While our earlier calculations [33] of experimental ENDOR spectra developed reliable values for the A matrices, it is hoped the new ENDOR simulations will give more reliable information on line intensities, and thus allow a better fit between simulation and experiment. An experimental and theoretical ENDOR spectrum of our first model compound, perylene, are shown in Figure 11.

Figure 11. Experimental (——) and theoretical (---) ENDOR spectra; perylene$^+$ radicals formed on activated alumina. T = 110K [16]

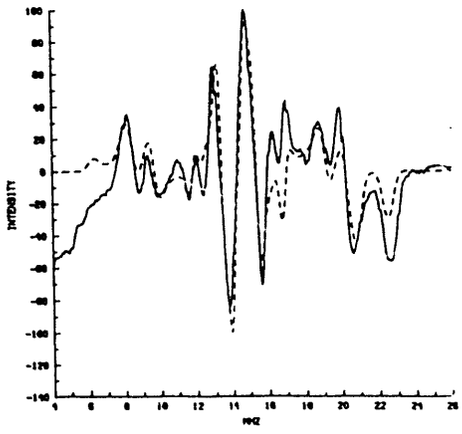

As we develop a more thorough understanding of the ENDOR spectral characteristics of radicals formed from model compounds, we continue to build a library of spectra on which to base the simulation of ENDOR and ESE spectra whole coal and separated macerals. Using the experimental and theoretical techniques developed for our work on perylene, we now are analyzing radicals formed from anthracene, naphthalene, pyrene, and dimethylanthracene. This selection of compounds should span a significant percentage of the aromatic hydrocarbon radicals found naturally in coal.

We also are studying dibenzothiophene and thianthrene in order to learn the characteristics of sulfur heterocycles thought to be important forms of organic sulfur in Illinois coals. We believe that this approach, using ENDOR to study intermolecular hyperfine interactions in model systems, affords us the most direct route to an improved understanding of the more complex spectra obtained from coal.

A detailed theoretical understanding of the proton hyperfine couplings in the radicals found in coal is needed if we are to use them to probe the molecular structure of organic sulfur. This is true for both ENDOR and ESE measurements. Most fundamental is the theory linking 1) a particular molecular geometry and bonding pattern and, 2) the hyperfine couplings observed by ENDOR or ESE spectroscopy. In order to develop this structural theory of hyperfine couplings for radicals that are models of coal composition, we have calculated the theoretical couplings in the perylene radical. Two methods were used. The first was developed by McConnell and Strathdee [34]. In this method, the isotropic hyperfine contribution to the spin Hamiltonian is simply made proportional to the π-electron spin density on the carbon. The anisotropic hyperfine interaction is approximated by a magnetic dipole interaction between the proton and an electron spin magnetization centered on the carbon in a p-orbital.

There are several problems with this method. First of all, the electron is not really in a p-orbital on an isolated carbon atom: it actually is delocalized in a π-orbital. Also, each electron - proton interaction is treated as a C-H fragment. Thus, in the McConnell-Strathdee treatment, the dipolar interactions of neighboring electron spin density is ignored. In spite of these problems, the method gives excellent qualitative and reasonable quantitative results when compared to the ENDOR experimental values.

In order to include interactions of the additional electron spin magnetization on the other carbons, the method of hyperfine calculation proposed by O'Malley and Babcock has been used [35]. The inclusion of these neighbor interactions caused substantial deviation from the values expected for an isolated C-H fragment. In this calculation, which we have just completed for the perylene radical, all carbon atoms with a spin density within 5 Å of the proton of interest have been included as point dipole interactions. The interaction of the proton connected directly to a carbon is approximated as an isolated C-H fragment and the other interactions are added after transformation to a common axis system. In addition to changing the hyperfine tensor components, inclusion of the additional interactions causes a rotation of the principal axis system. In the original system, the y-axis is taken as the C-H bond, the x-axis is perpendicular to it in the plane, and the z-axis is out of the plane of the molecule. With the inclusion of neighbor interactions, the axis system is rotated for each proton, the effect being most pronounced for the ß-proton, which has the smallest spin density on its bonded carbon.

The analysis of coal macerals has posed a problem with resolution when using EPR spectroscopy. Coal samples examined at the traditional X-band microwave excitation frequency typically exhibit a single, nearly symmetric EPR absorption line that is too featureless to analyze uniquely. At W-band (95 GHz) however, anisotropic interactions in the g-matrix become apparent. The first W-band EPR experiment on coal unambiguously revealed the axial character of the system. The anisotropy of the g-matrix increases the chance of arriving at a unique theoretical description of the coal system.

In order to properly simulate the spectra obtained from coal-derived samples it becomes necessary start from fundamental building blocks of information. Sulfur containing systems inside coal are of special interest because of the concern over high

sulfur content. Information about simpler sulfur-containing molecules is needed to use in assembling the simulated spectra for coal samples. Thiophenes become the focus of this research effort because most organic sulfur inside coal is in the form of thiophenes.

It was necessary to develop a consistent method to analyze the spectra obtained from the model systems with the emphasis on the anisotropic effects upon the EPR spectrum caused by sulfur. Thianthrene, a sulfur containing heterocyclic compound was a good model to begin with because it displays observable anisotropic features attributable to g-matrix anisotropy in its X-band EPR signal when it is adsorbed onto the silica-alumina surface. Through the analysis of thianthrene's complex EPR and ENDOR spectra an analytical method of simulating disordered solid systems was developed. Since the anisotropic interactions in thianthrene are very complex, the method is applicable to highly disordered systems in general and systems with less anisotropy. The focus of future experiments will be to apply this developed method to thiophenes. We plan to characterize several thiophene class compounds that resemble the possible configurations of sulfur in coal.

Improvements must still be made on sample preparation techniques in order to obtain reproducible and reliable data from the analysis of the model systems. New surface treatment methods are currently being attempted to increase the EPR and ENDOR signals.

The model system that worked best for the thianthrene experiment was produced by first calcining Houdry-M46 brand silica-alumina under vacuum and introducing the thianthrene in the gas phase. The samples were prepared in quartz X-band EPR sample. EPR was performed on a Varian 12" Century Series EPR spectrometer with ENDOR capabilites. ENDOR spectra were taken at incremented magnetic field positions within the field range covered by the EPR signal.

The g-matrix was obtained by fitting the experimental EPR spectrum with a computer generated EPR spectrum. The parameters were optimized by using a auto-iterative routine that minimizes a least squares response function. The hyperfine matrices were obtained by optimizing the fit between the experimental ENDOR spectra and computer generated ENDOR spectra at various field positions.

Figures 12 and 13 show results. Figure 12 compares the experimental EPR spectra and the best fit calculated by the method of Belford (Ref.[1]). The parameters are g[1] =

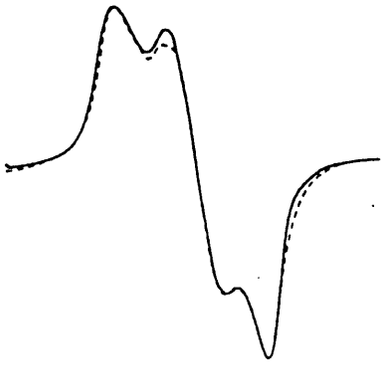

Figure 12. EPR spectrum of thianthrene (+). Experimental (_____); theoretical (---).

2.00146, g[2] = 2.00744, g[3] = 2.01261. Figure 13 compares experimental to calculated ENDOR spectra at the three field positions. There is a clear shift in hyperfine frequencies and intensities observed between the extreme field values. The distribution of molecular orientations relative to applied magnetic field contributing to the ENDOR spectrum varies with field. That is, there is some angle selection at X-band although there is considerable overlap between the 3 turning points of the EPR spectrum. The best fit of the ENDOR spectra at all three field values required the assigning of the diagonal matrix g-values to be g[x] = 2.00744, g[y] = 2.01261, g[z] = 2.00146.

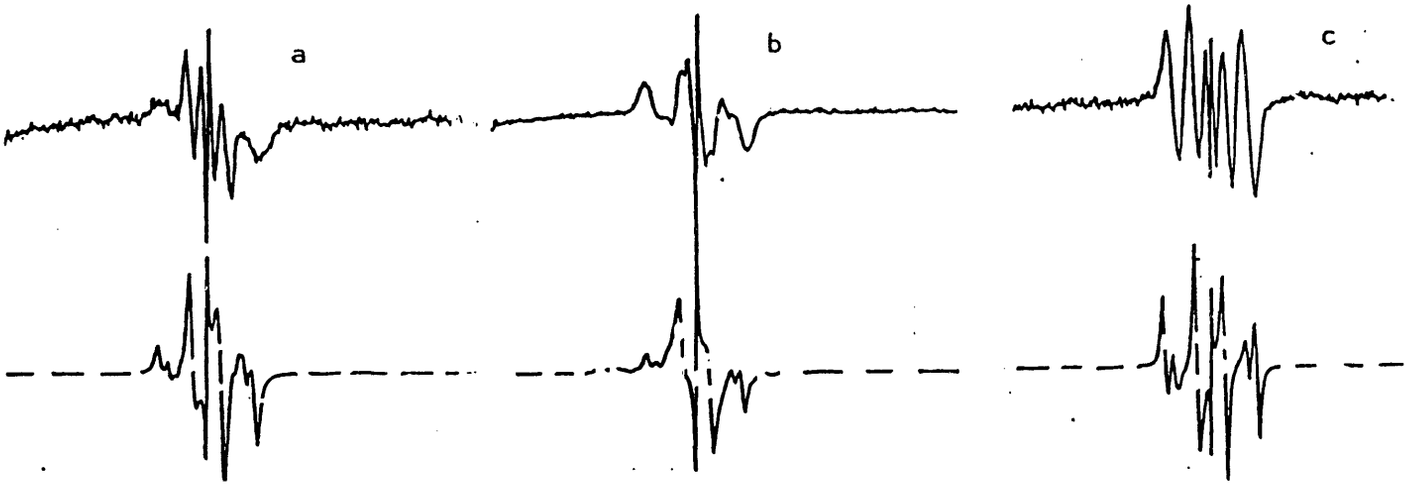

Figure 13. "Orientation selection" in proton ENDOR of thianthrene at three field positions. Experimental (_____), theoretical (---).

One conclusion that can be drawn is the assignment of the diagonal g-matrix elements g[x], g[y], g[z] to the quantitative values calculated for the system and the consequent assignment of the directions of the g-values relative to the molecular geometry of the bound thianthrene. Figure 14 shows the present assignment for the directions of the numerical g-values. We must improve our calculation and continue refining the ENDOR parameters in order to be certain of this conclusion and to draw new conclusions about the model system.

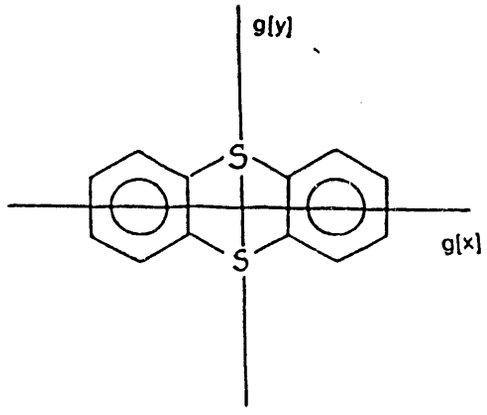

Figure 14. Assignment of directions of the cannonical g-values in thianthrene.

The analysis described must be completed for thiophene compounds since thiophenes are better models for sulfur centers in coal. The preparation of thiophene models have been slightly more difficult in the past but have improved recently and better spectral signal to noise has been obtained. The computer algorithm used could also be improved by adding higher order correction terms to the spin Hamiltonian.

Hardware and software have been developed to allow us to perform automated 2-dimensional ENDOR experiments on coal and separated maceral samples. The most conventional form of 2-D experiments involves RF frequency and magnetic field as the two variables, although RF power, temperature, microwave power, receiver phase, and modulation frequency are other variables we have used. Figure 15(a) illustrates a simple 2-D ENDOR spectrum of a charred sucrose sample, showing a single matrix

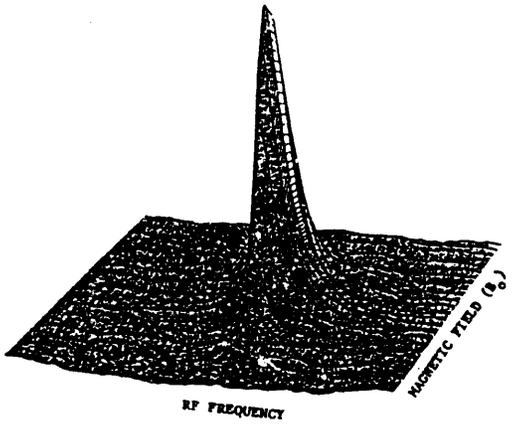

Figure 15(a) 2-D ENDOR of charred sucrose sucrose at 300K.

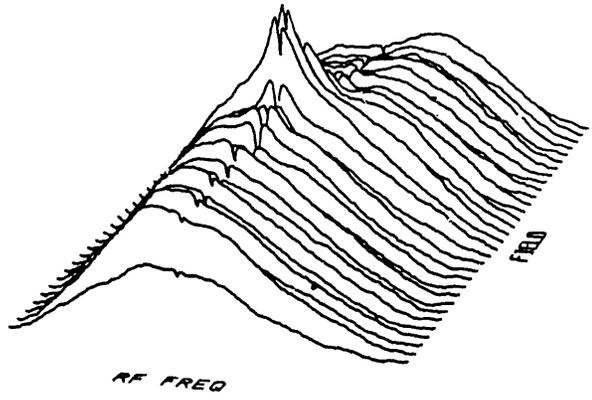

Figure 15(b). 2-D ENDOR of Illinois #6 coal at 150K.

peak maximum. Such artistic plots become impossible to interpret when spectra become complex, as can be seen in Figure 15(b) showing the 2-D ENDOR of an evacuated Illinois #6 whole coal, and contour plots are then more useful. Figure 15(c) shows a contour plot of the data in 15(b).

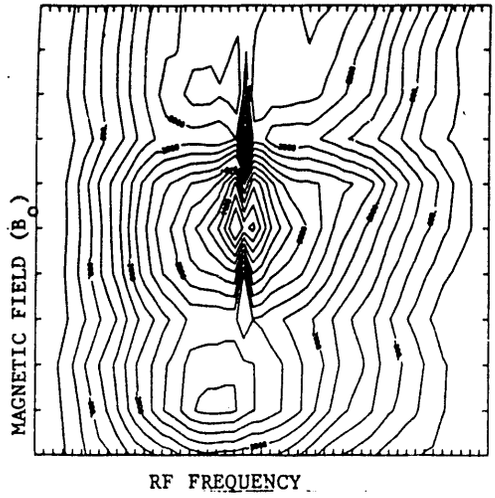

Figure 15(c). 2-D ENDOR contour plot from Illinois #6 coal at 150K.

Two very important results have emerged from our first 2-D ENDOR work on coal.

The first is that contour plots allow the assessment of **patterns** or correlations just as in 2-D NMR. Peaks occurring along field lines (or g-lines) can be correlated and analyzed. This can be seen in Figure 15(d), where a set of peaks at a g-value lower than the "center" g-value appear. It may be that these peaks arise from a

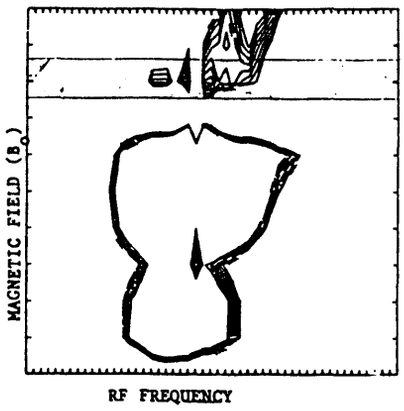

Figure 15(d). Expansion of 15(c) showing g-value correlated peaks.

functional group or groups with fewer heteroatom interactions. 2-D ENDOR allows us to see these peaks **as patterns**, and it also **improves resolution**. When these experiments are performed at higher fields (Q- and W-band), the greater field dispersion will make resolution enhancement even more dramatic.

The second very important result to come from our first 2-D ENDOR work is the observation of significant dynamic nuclear polarization (DNP) effects in the ENDOR spectra. Figure 16 shows the field profile (or ENDOR-induced EPR) of a 2-D data set taken from an Illinois #6 fusainite. (One of the additional features of 2-D experiments is that it allows the construction of "slices" like this through the spectral surface along any field or frequency line.) The ENDOR-induced EPR spectrum in this absorption display should be everywhere positive, yet this data shows tremendous **positive and negative** peaks due to

Figure 16.
Field profile of 2-D ENDOR data along the 15MHz line showing DNP in a fusainite.

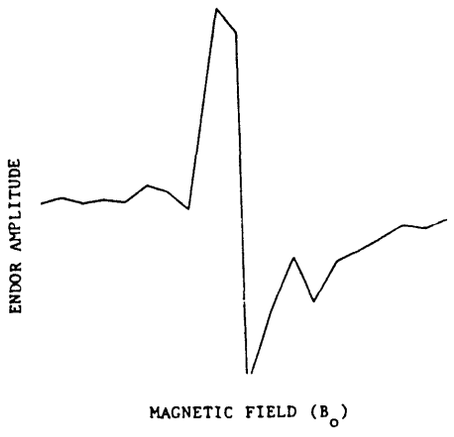

a "solid state effect" DNP. While this is interesting in itself, it is not the focus of our research. Rather, it causes us to remember the theory suggesting that DNP and ENDOR are in a sense **competing effects**, and that significant loss of ENDOR resolution will be observed in systems showing DNP if the RF (ENDOR) excitation is not strong enough to overcome polarization pathways. We have always been puzzled why the original ENDOR results of Retcofsky, et. al. showed resolution not achieved by other ENDOR experiments, and why ESE gives such better resolution than ENDOR in the same coal samples. Our 2-D ENDOR results showing DNP suggest an answer to the puzzle and point out the direction our work should take:

1. Retcofsky's work was performed on a high power Varian ENDOR instrument with a tuned RF coil, achieving 50-60G fields in the rotating frame (B_2), while subsequent work by ourselves and others has been on broadbanded spectrometers developing B_2 fields of 10-15G. These lower B_2 fields are sufficient to reveal ENDOR effects, **but not strong enough to overcome DNP competition** in relaxation pathways;
2. DNP effects appear on a **nuclear T_1 timescale**, requiring many milliseconds of microwave irradiation, while ESE experiments are performed on an **electronic T_1 timescale**, with microwave pulses of nanoseconds. Thus, in the ESE experiments, the microwave field is not on long enough to allow DNP effects to build. Conversely, in cw ENDOR experiments, the microwave field is on continuously, maximizing DNP effects and reducing spectral resolution.

This entire discovery, which was not made until the advent of 2-D ENDOR, suggests that to improve spectral resolution in coal we need to:

1. Use pulsed microwave techniques;
2. Use either very strong B_2 fields in cw ENDOR, or work at higher field strengths where the "forbidden" cross transitions responsible for DNP will be minimized.

We are working on all of these approaches now.

3) Pulsed S-band EPR and ESE

If ENDOR spectroscopy is the method of choice for the resolution of strong hyperfine interactions, ESE is uniquely sensitive to weaker, intramolecular interactions. In the first published account of ESE measurements in coal, Kevan, et. al. studied matrix proton interactions, calculating a mean distance between unpaired electrons and protons in an SRC of $r = 0.5 \pm 0.03$ nm, and an apparent interaction shell occupancy of $n = 16 \pm 2$ protons [13]. Das, et. al. found a value of $r = 0.36 \pm 0.04$ nm (n not reported) from a similar analysis of two-pulse ESE experiments performed on a low-sulfur Pittsburgh bituminous coal [36]. The matrix interaction, it will be remembered, is the essentially electron-nuclear dipole-dipole coupling between non-bonded atoms, and thus reflects the density of nuclei in the immediate **neighborhood** of the unpaired electron. The model used for these first analyses was a spherical shell, depicted in Figure 17. Such information, when correlated with specific maceral types, should provide us with a much more precise measurement of the atomic structure of coal, and may be diagnostic of structural changes brought about by various coal beneficiation technologies.

We have performed experiments on powdered Illinois #6 whole coal using a three-pulse ESE sequence, and have analyzed the matrix ESEEM by the spherical shell model. Figure 18 shows our data and best-fit simulation using $r = 0.75 \pm 0.05$ nm and $n = 40$ protons [6]. Variations in r and n among the three reported measurements may be due to differences in the structure of the samples studied; more likely sources of variations are the differences in experimental techniques (two-pulse, three-pulse), and different spectrometer characteristics (pulse power, cavity Q, etc.) used in the three studies. We

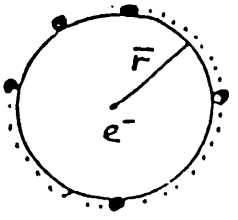

Figure 17. The spherical shell model for analysis of matrix ESEEM.

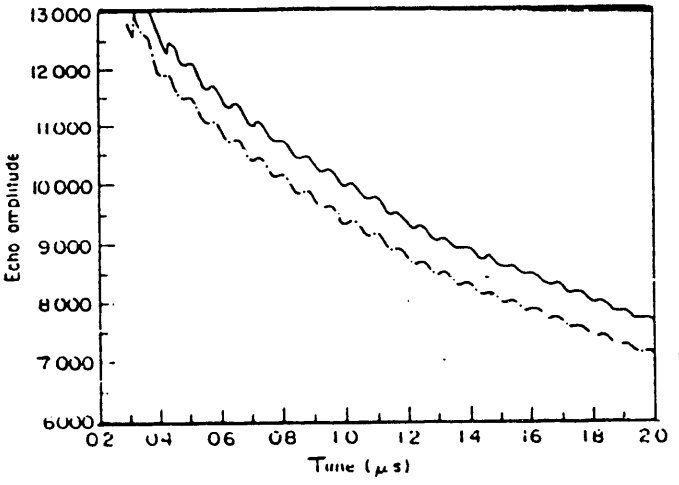

Figure 18. X-band ESEEM data, experimental (———) and theoretical (-----) for an Illinois #6 whole coal [6].

currently are making a detailed study of these effects using whole coals and coal model systems in an effort to better understand the role of experimental factors in the results obtained. We also are studying the utility of more realistic model geometries (eg, layered structure) and the sensitivity of ESEEM simulations to the choice of geometry.

In 1984, we first reported the observation of matrix ESEEM from ^{13}C nuclei in natural abundance in coal [37]. Since that time, we have worked to understand the experimental and theoretical characteristics of this important effect, and we have recently developed criteria to optimize experimental sensitivity [38]. Because, to zeroth order, ESE sensitivity does not depend on the nuclear gyromagnetic ratio, this spectroscopy is much better suited for the observation of "low gamma" elements such as carbon and sulfur, which present severe problems for ENDOR and NMR. Data on ^{13}C ESEEM thus far suggests that in an Illinois #6, r = 0.31 ± 0.01 nm, and n = 2. Clearly, the opportunity to map the carbon skeleton of coal with this technique represents a great opportunity; it also is clear that much more work is needed to fully understand and correctly interpret such data.

Measurements on a vitrinite separated from the Illinois #6 also have been made, employing both short, hard pulses (40 nsec = $\pi/2$) and long, soft pulses (200 nsec = $\pi/2$). The long pulses have very narrow frequency bandwidths, exciting only those transitions corresponding to the weakest dipolar couplings between electrons and distant protons, while the short pulses excite a wider range of transitions. By dividing the long, selective pulse data into the more non-selective, short pulse data removes the "background protons" from the experimental results, allowing a more detailed examination of the stronger hyperfine couplings. Work on this technique is continuing,and promises to provide more tractable data sets for the study of coal maceral molecular structure.

Employing a two-pulse echo sequence, we have measured the phase memory times (T_M) of coals in the Argonne Premium Coal Sample bank. The results of these

measurements are summarized in Table II.

Table II. Electron Spin Echo Decay Times, T_M, for Argonne Premium Coal Samples at 4.0 GHz and Several Magnetic Fields

Argonne Sample	Field (G)	T_M (nsec)
101	1436	626
101	1449	821
101	1434	681
301	1434	534
301	1440	563
401	1440	525
401	1450	665
501	1442	493
501	1452	394
601	1432	378
601	1437	402
601	1442	379
601	1447	352
801	1398	341
801	1416	297

It can be seen from the data that field position (B_o) has an important effect on the value of T_M that is obtained. This strongly suggests that different maceral components in many of these coals have different phase memory times, and that pulsed measurements can be very sensitive to these differences. Such sensitivity may provide a method of obtaining information on individual macerals from a whole coal in a non-destructive manner.

4) Computer-aided simulation

Spectral parameters of EPR and related types of spectra are typically obtained by simulating the experimental spectrum. Trial and error fitting of the spectral parameters can be time consuming and difficult especially if there are many adjustable spectral parameters and overlapping features. Often, as a result, the number of spectra that are feasible to simulate is severely limited, and it is difficult to arrive at a satisfactory fit. This is especially true of the ENDOR spectra of coal model systems. This has led us to develop a method to assist in the fitting of simulation parameters.

We have designed a procedure to automate the fitting of spectral parameters in simulations. Each trial simulation is mathematically compared to the experimental spectrum and a new set of trial spectral parameters is chosen based on the results of all the previous simulations in the optimization. This process continues until a satisfactory simulation is obtained. The spectral parameters are chosen according to the simplex method of optimization. This method was chosen for use because its flexibility makes the program applicable to a variety of spectra. Thus, the fitting procedure can be used with any of our simulation programs to optimize the spectral parameters of EPR, ENDOR, and ESEEM spectra.

Our goal is to use the optimization procedure routinely in the course of our data analysis both as a time saving device and as a way to insure that the most accurate spectral parameters result from our simulations.

The automation procedure which we have developed makes use of the simplex method of optimization. Simplex optimization can be used to vary any number of parameters to find the set of values which gives the optimum response. The response is a function of the parameters which quantifies the results at each set of parameter values. The optimum is the maximum or minimum of the response function, depending on how it is defined. In this case the parameters are the variables in the simulations, the response is some measure of the match between the experimental spectrum and the simulation created with the set of parameter values that correspond to the vertex whose response is being measured, and the optimum would represent the values of the parameters leading to a simulation as nearly identical as possible to the experimental spectrum.

The simplex method employs an n-dimensional polyhedron, where n is the number of variables being optimized. This polyhedron, called a simplex, has n + 1 vertices, each having n coordinates which represent values of the variable parameters. For example, the simplex for an optimization of two variables (x,y) is a triangle in which each of the three vertices has two coordinates which represent values of the two variables - i.e., (x_1,y_1), (x_2,y_2), (x_3,y_3); the simplex for a three-variable optimization is a tetrahedron, and so on. After the initial simplex is determined, the response at each vertex is measured. The vertex with the worst response is replaced by its reflection through the hyperface of the remaining vertices. The response at the new vertex is measured and again the worst vertex is replaced. Repetition of this process causes the simplex to move over the response surface in the direction of the optimum as illustrated in Figure 19 for an optimization of two variables.

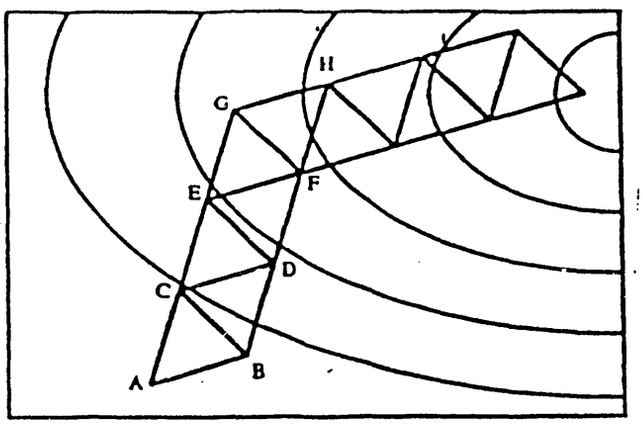

Figure 19: Movement of the simplex method on a two variable response surface. ABC is the initial simplex. The vertex with the worst response, A, is replaced by its reflection, D. The simplex proceeds towards the optimum by replacing B with E, C with F, and D with G.

The modified simplex method was used in this project. It allows the worst vertex to

be replaced not only by a reflected vertex but also by vertices that represent an expansion or contraction of the simplex. This allows the simplex to adjust its size in order to move more rapidly towards the optimum.

The response function used in the procedure can include any number of terms which quantify the goodness of fit between the experimental spectrum and the simulation. A least squares response provides a measure of the overall fit of the simulation. It is the sum over the data points of the squares of the differences between the experimental and simulated intensities. We have used this term as a response function both on its own and in combination with other terms which quantify how well the simulation reproduces the extrema of the experimental spectrum.

We have used the optimization procedure with a number of our simulation programs. Included are the simulations of EPR powder spectra, ENDOR spectra with isotropic and anisotropic g-values, and ESEEM spectra. It has been shown to provide us with accurate spectral parameters in a fraction of time previously needed for simulation. We are now able to more routinely simulate complicated spectra such as the ENDOR spectra that we obtain on polycyclic and polynuclear aromatic cations, our model systems for coal.

5) MRI imaging of coal

The first proton images of coal have been made through the collaboration of Dr. Paul Lauterbur and the Biomedical Magnetic Resonance Laboratory (BMRL). A sample of Illinois #5 (Galatin County) or #6 (Herrin County) was placed in a glass bottle 3.2 cm in diameter. The bottle first was filled with water doped with 1 mM $MnSO_4$ to shorten the longitudinal relaxation time (T_1 = 400 msec for the doped water). Proton NMR of the water revealed a proton peak with $\Delta\nu_{\frac{1}{2}}$ = 171 Hz. Images then were made utilizing the water protons as the imaging medium.

Figure 20 shows three 1 mm thick slices through a piece of Illinois #5. The bright channels are internal pore structures, and are not cracks in the coal.

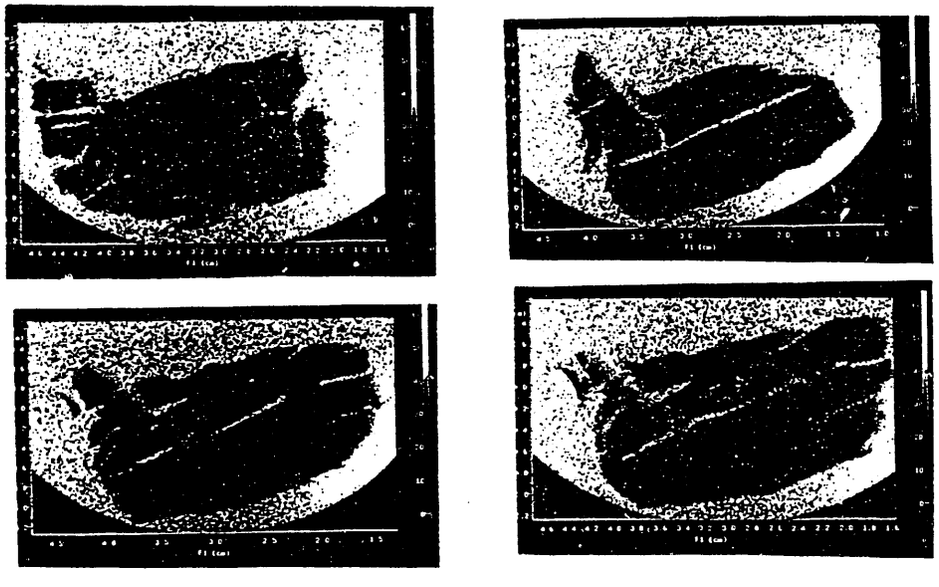

Figure 20. 1 mm MRI slices through a piece of Illinois #5 immersed in water.

The water then was removed from the coal and was replaced with acetone doped with 10 mM $Cr(AcAc)_3$. Again, proton images were made with the acetone protons. Finally, the acetone was removed and replaced with DMSO doped with 10 mM $Cr(AcAc)_3$. Proton images of the same piece of Illinois #5 in acetone and DMSO are shown in Figure 21.

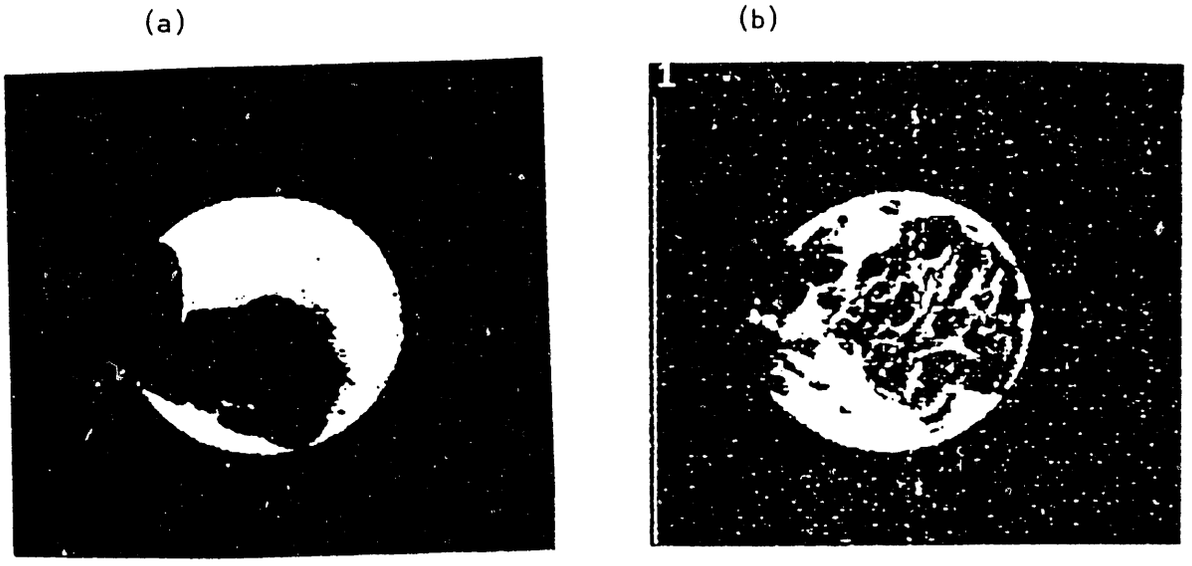

Figure 21. Proton MRI images of the interior of a piece of Illinois #5 in (a) acetone; and (b) DMSO.

The images in Figure 21 clearly show the significant pore enlargement and swelling of the coal in DMSO. To obtain information on the swelling ratio, Q, defined as the ratio of coal volumes in different solvents, we cut out and weighed the images of the coal in acetone and DMSO. This ratio, 1.556, is the ratio of the cross sectional areas of the coal in the two solvents. Assuming a spherical model, we can calculate the volume ratio, which is 1.9. This represents the value of $V_{DMSO}/V_{Acetone}$. In a hvB coal, this ratio for the two solvents we used has been measured to be 1.6 [39]. It is clear than, that MRI represents a powerful new approach to the study of solvent penetration and swelling in coal.

Current work is focussing on developing higher resolution images of coal in order to determine the dependence of solvent penetration on maceral type. Images obtained from optical microscopy at the Illinois State Geological Survey are being digitized and compared to the MRI images to map the distribution of maceral types. This information will give the first detailed picture of the accessibility of different characterized regions of a piece of coal to different solvents, and will help to better describe processes like solvent extraction.

6) Oxygen adsorption in fusinite

In the course of our VHF EPR study of coal, we noted the unique signal observed

from fusinite macerals. In particular, the very strong effect of gaseous oxygen on the width of this resonance line led us to speculate whether this interaction could be calibrated and used as a means of measuring oxygen pressure. In order to learn more about the process, we constructed a vacuum system that allows us to vary the pressure of gaseous oxygen on a sample of vitrinite while it is positioned in an EPR spectrometer. By measuring EPR spectra of a separated vitrinite under different oxygen pressures (P_{OXYGEN}), we were able to follow changes in the spectral linewidth, ΔH_{pp}; the results of these measurements are shown in Figure 22.

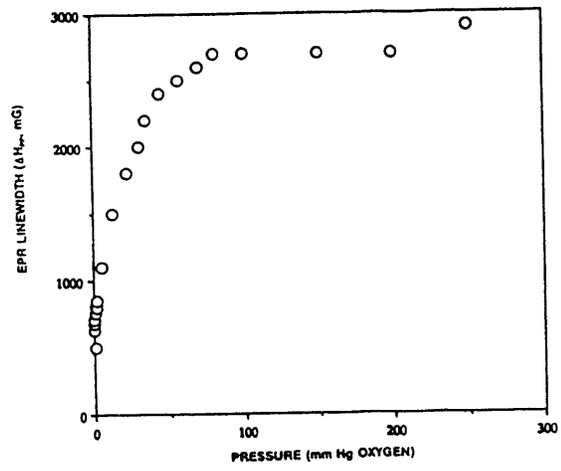

Figure 22. Variation of ΔH_{pp} as a function of P_{OXYGEN} in a fusinite separated from Illinois #6.

The overall shape of the curve looks like a Langmuir-type isotherm, and suggests that the adsorption of oxygen in the pores of fusinite is responsible for the line broadening. Such curves are reversible and precisely reproducible.

Pulsed EPR of evacuated fusinite at 4 GHz produced the strong FID shown in Fig. 23 and no detectible spin echo, suggesting that the line is very homogeneous in the absence of oxygen. Experimental details of this measurement have been described elsewhere [4].

FID's collected in the presence of oxygen were much weaker, and disappeared at P_{OXYGEN} greater than about 100 mm Hg. Simulation of the FID's using a series expansion of exponentially damped sinusoids allowed the determination of the phase memory time, T_M, as a function of oxygen pressure, as shown in Fig. 24. T_M does not behave like ΔH_{PP} in this pressure region (see Fig. 22), and strongly suggests that the mechanism for line broadening by oxygen in fusinite has an important inhomogeneous component. This hypothesis is further strengthened by preliminary data on the behavior of T_{1e} as a function of oxygen pressure.

---

[4] Clarkson, R. B., Timken, M. D., Brown, D. R., Crookham, H. C., and Belford, R. L., Chem. Phys. Lett., 163, 277 (1989).

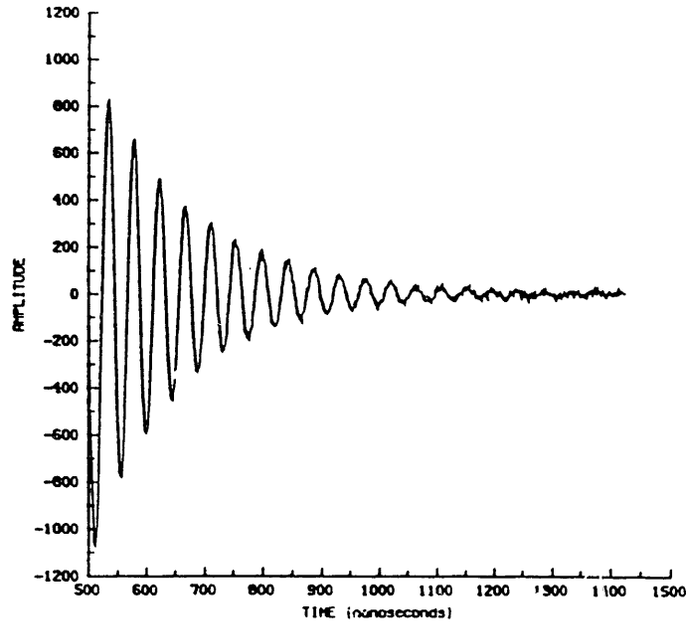

Figure 23. Electron FID from evacuated fusinite at 4 GHz obtained by pulsed EPR at room temperature.

These measurements suggest that there are two classes of unpaired electrons in this system: (1) a pool of delocalized, exchange coupled electrons, and (2) more localized, surface unpaired spins. Type 1 electrons are the predominate form in evacuated fusinite, and Type 2 electrons are formed from Type 1 as oxygen adsorbs on the surface. The FID's measured in fusinite are therefore a manifestation of Type 1 electrons.

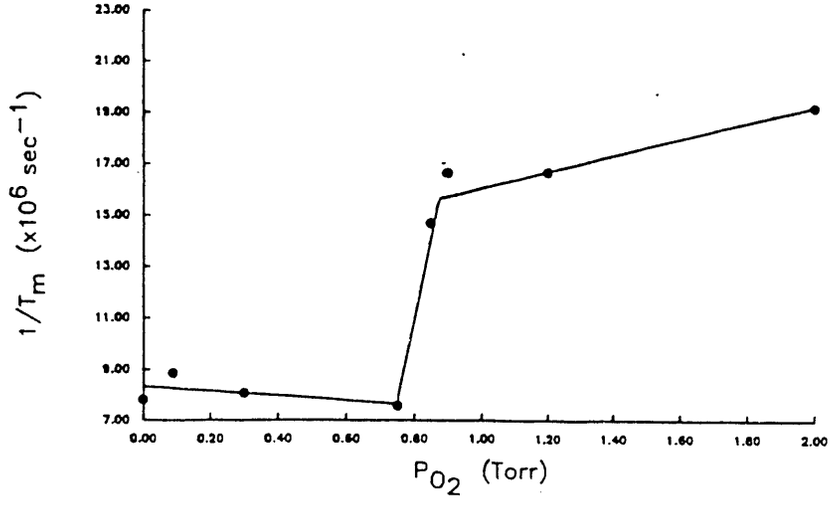

Figure 24. The variation of T_M with oxygen pressure in fusinite at room temperature.

Temperature affects the value of ΔH_{PP} observed in fusinite at any pressure of oxygen, and measurements are currently under way to determine EPR linewidth as a function of P_{OXYGEN} at different temperatures. In the course of these experiments, oxygen was admitted to a sample of fusinite that had been evacuated and cooled to -170 C. No

line broadening was observed, so the temperature was carefully increased, resulting in the curve shown in Fig. 25. ΔH_{PP} for fusinite as a function of temperature in the absence of oxygen also is plotted for comparison. The temperature dependence of the line broadening may reflect an activation energy for the process, or it may be the result of essentially surface effects such as capillary condensation of oxygen in the micropores of the fusinite at low temperatures.

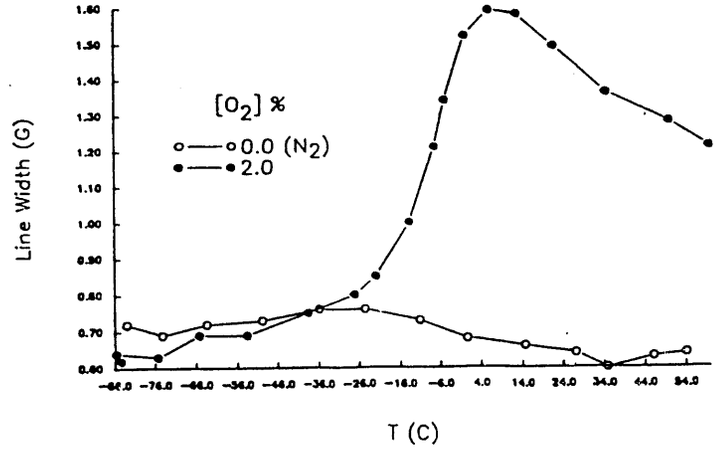

Figure 25. The temperature dependence of ΔH_{PP} in fusinite after the introduction of O_2 to an evacuated sample at -170C.

The temperature dependence of the rate of line broadening following the administration of a sudden dose of oxygen also is being studied. Fig. 26 shows data for room temperature, and illustrates that equilibration is more rapid for a rise in oxygen pressure (ΔH_{PP} increases, and signal height decreases, with time) than for a fall in pressure. Thus, according to our model, oxygen adsorption is a more rapid process than desorption, which agrees with typical chemisorption mechanisms.

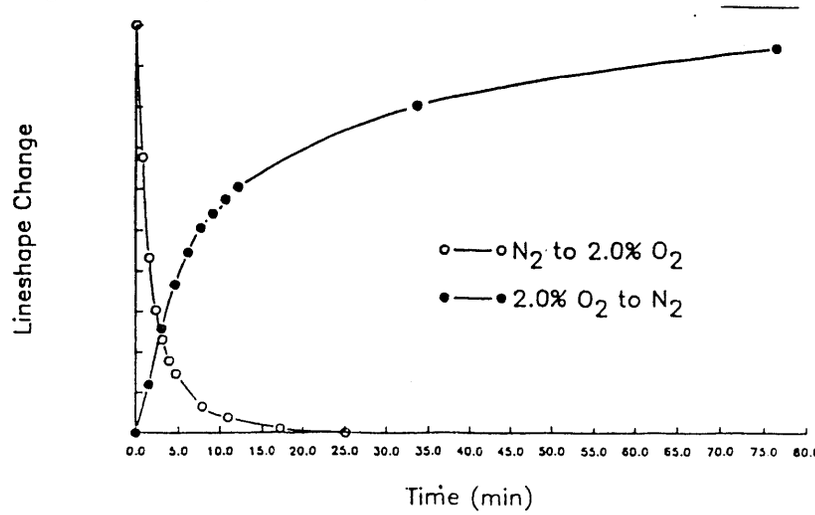

Figure 26. Time dependence of the signal height of fusinite following increase or decrease in oxygen concentration. $t_{\frac{1}{2}}$ (adsorption) = 1.4 minutes; $t_{\frac{1}{2}}$ (desorption) = 7.7 minutes at room temperature.

Conclusions from our study of oxygen effects in fusinite thus far can be summarized as follows:

1. Fusinite has an EPR linewidth that is reproducibly affected by oxygen pressure or concentration in solution.
2. Fusinite signals appear to be broadened by an inhomogeneous mechanism related to the chemisorption of oxygen on the microporous surface of the maceral.
3. Fusinite has a value of $d\Delta H_{PP}/dP_{OXYGEN}$ that is very much larger than that measured for nitroxides, the class of compounds currently being used to measure oxygen concentration by and thus represent two attractive new chemical probes for in vivo EPR oximetry.

REFERENCES

1. W. H. Wiser and R. H. Wolk, ACS Fuel Div. Prepts., 20 (2), 122 (1975).

2. R. M. Davidson, Molecular Structure of Coal, IEA Coal Research, London, 1980.

3. J. H. Shinn, FUEL, 63, 1187 (1984).

4. L. Lazarov and S. P. Marinov, Fuel Proc. Technol., 15, 411 (1987).

5. K. J. Hüttinger and A. W. Michenfelder, FUEL, 66, 1164 (1987).

6. J. Uebersfeld, A. Etienne, and J. Combrisson, Nature, Lond., 174, 615 (1954).

7. D. J. E. Ingram, J. G. Tapley, R. Jackson, R. L. Bond, and A. R. Murnagham, Nature, Lond., 174, 797 (1954).

8. H. L. Retcofsky, M. R. Hough, M. M. Maguire, and R. B. Clarkson, in Coal Structure, M. L. Gorbaty and K. Ouchi, eds., ACS Advances in Chemistry, 192, ACS, Washington, 1981, pp. 37 - 58.

9. R. B. Clarkson, R. L. Belford, K. S. Rothenberger, and H. C. Crookham, J. Catalysis, 106, 500 (1987).

10. R. B. Clarkson, R. L. Belford, J. B. Cornelius, P. A. Snetsinger, and M. K. Bowman, FUEL, 66, 925 (1987).

11. L. Kevan and R. N. Schwartz, Time Domain Electron Spin Resonance, John Wiley & Sons, New York, 1979.

12. K. Ohno and T. Yokono, Carbon, 24, 517 (1986).

13. L. J. Berliner, H. Fujii, X. Wan, and S. J. Lukiewicz, Mag. Res. Med., 4, 380 (1987).

14. M. M. Maltempo, S. S. Eaton, and G. R. Eaton, J. Mag. Res., 72, 449 (1987).

15. Schlick, S. and Kevan, L., in Magnetic Resonance. Introduction, Advanced Topics, and Applications to Fossil Energy., Petrakis, L. and Fraissard, J. P., Eds.; D. Reidel: Dordrecht, 1984; p. 655.

16. Malhotra, V. M., and Buckmaster, H. A., Org. Geochem., 1985, 8, 235.

17. Belford, R. L., Clarkson, R. B., Cornelius, J. B., Rothenberger, K. S., Nilges, M. J. and Timken, M. D. In Electron Magnetic Resonance of the Solid State, Weil, J. A., Ed.; Chemical Institute of Canada: Ottawa, 1987, p 21.

18. Clarkson, R. B., Wang, W., Nilges, M. J., and Belford, R. L. In Processing and Utilization of High-Sulfur Coal; Markuszewski, R. and Wheelock, T. D., Eds; Elsevier: New York, 1990.

19. Hurst, G. C., Henderson, T. A., and Kreilick, R. W., J. Am. Chem. Soc. 1985, 107, 7294.

20. Clarkson, R. B., Timken, M. D., Brown, D. R., Crookham, H. C., and Belford, R. L. Chem. Phys. Letters 1989, 163, 277.

21. Flanagan, H. L., and Singel, D. J. J. Chem. Phys. 1987, 87, 5606.

22. Cornelius, J. B., McCracken, J., Clarkson, R. B., Belford, R. L., and Peisach, J. J. Phys. Chem., 94, 6977 (1990).

23. Lai, A., Flanagan, H. L., and Singel, D. J. J. Chem. Phys. 1988, 89, 7161.

24. Vorres, Karl S. Users Handbook for the Argonne Premium Coal Sample Program; Argonne National Laboratory: Argonne, 1989.

25. Lynch, W. B., Earle, K. A., and Freed, J. H. Rev. Sci. Instrum. 1988, 59, 1345.

26. Clarkson, R. B., Belford, R. L., Rothenberger, K. S., and Crookham, H. C. J. Catalysis 1987, 106, 500.

27. Silbernagel, B. G., Gebhard, L. A., and Dyrkacz, G. R., In Magnetic Resonance. Introduction, Advanced Topics, and Applications to Fossil Energy. Petrakis, L. and Fraissard, J. P., Eds.; D. Reidel: Dordrecht, 1984; p. 645.

28. Stone, A. J. Mol. Phys. 1964, 7, 311.

29. Attar, A. and Dupuis, F. Am. Chem. Soc. Div. Fuel Chem. Preprints. 1979, 24, 166.

30. S. Schlick, M. Narayana, and L. Kevan, J. Am. Chem. Soc., 100, 3322 (1978).

31. H. L. Retcofsky, M. R. Hough, M. M. Maguire, and R. B. Clarkson, Coal Structure, eds. M. L. Gorbaty and K. Ouchi, ACS Advances in Chemistry, 192, ACS, Washington, 1981, pp. 37 - 58.

32. L. R. Dalton and A. L. Kwiram, J. Chem. Phys., 57, 1132 (1972).

33. R. B. Clarkson, R. L. Belford, K. S. Rothenberger, and H. C. Crookham, J. Catalysis, 106, 500 (1987).

34. H. M. McConnell and J. Strathdee, Mol. Phys., 2, 129 (1959).

35. P. J. O'Malley and G. Babcock, J. Am. Chem. Soc., 108, 3995 (1986).

36. U. Das, D. C. Doetschman, P. M. Jones, and M. Lee, FUEL, 62, 285 (1983).

37. "The Interactions of Paramagnetic Centers with ^{13}C, ^{1}H, and Adsorbed Oxygen in Coal," R. B. Clarkson and M. K. Bowman, 7th International EPR Symposium, Denver, 1984, paper no. 87.

38. P. A. Snetsinger, J. B. Cornelius, R. B. Clarkson, M. K. Bowman, and R. L. Belford, J. Phys. Chem., 92, 3696 (1988).

39. J. Szeliga and A. Marzec, FUEL, 62, 1229 (1983).

B. Bibliography of publications from this project

(Note: Publications (including Abstracts and Dissertations) resulting either wholly or partly from the DOE grant or acknowledging it. Most listed have publication dates in 1988 or later, when the current DOE funding started; a few with earlier publication dates are derived from the preceding DOE funding period.)

"ENDOR of Perylene Radicals Adsorbed. II. The Matrix Effects," K. Rothenberger, H. Crookham, R. L. Belford, and R. B. Clarkson, J. Catalysis, 115, 430-440 (1989).

"Influence of Organic Sulfur in Very High Frequency EPR of Coal", R. B. Clarkson, Third Processing and Utilization of High-Sulfur Coals, Ames, November, 1989; Clarkson, R. B., Wang, W., Nilges, M. J., and Belford, R. L. In Processing and Utilization of High-Sulfur Coals III; Markuszewski, R. and Wheelock, T. D., Eds; Elsevier: New York, pp. 67-79, 1990.

"Enhancement of Nuclear Modulation in Electron Spin Echoes at Low Magnetic Fields: S-Band ESE Spectrometer," Clarkson, R. B., Timken, M. D., Brown, D. R., Crookham, H. C., and Belford, R. L. Chem. Phys. Letters, 163, 277-281, 1989.

"Anisotropic EPR Spectra of Heterocyclic Sulfur Compounds," Dennis J. Youn, PhD Thesis, University of Illinois, Urbana, IL (1989).

"Studying Coal Molecular Structure with Electron Spin Echo Spectroscopy," R. B. Clarkson, R. L. Belford, J. Cornelius, and P. Snetsinger, Am. Chem. Soc. Fuel Div. Prepr., 31, 214 (1986).

"EPR Over Three Decades of Frequency: Radiofrequency to Infrared", R. L. Belford, R. B. Clarkson, J. B. Cornelius, K. S. Rothenberger, M. J. Nilges, and M. D. Timken, in Electron Magnetic Resonance of the Solid State, J. A. Weil, ed., Chemical Institute of Canada, Ottawa, 1987.

"ENDOR of Perylene Radicals Adsorbed on Alumina and Silica-Alumina Powders. I. The Ring Protons," R. B. Clarkson, R. L. Belford, K. Rothenberger, and H. Crookham, J. Catalysis, 106, 500 (1987).

"Electron Spin Echo Spectroscopy: A Tool to Probe Structural Properties of Coal," R. B. Clarkson, M. K. Bowman, J. Cornelius, P. Snetsinger, and R. L. Belford, FUEL, 66, 925 (1987).

"Electron Spin Echo Envelope Modulation by Natural Abundance Carbon-13 and Aluminum-27 in Two Disordered Systems", P. A. Snetsinger, J. B. Cornelius, R. B. Clarkson, M. K. Bowman, and R. L. Belford, J. Phys. Chem., 92, 3696 (1988).

"Multi-Frequency EMR Studies of Argonne Premium Coal Samples," R. B. Clarkson, W. Wang, D. L. Brown, H. C. Crookham, and R. L. Belford, in Techniques in Magnetic Resonance for Carbonaceous Solids, R. Botto and Y. Sanada, eds., ACS Advances in Chemistry Series, American Chemical Society, Washington, 1990 (in press).

"Multi-Frequency EPR Studies of Argonne and Illinois Sample Bank Coals," R. B. Clarkson, Wei Wang, D. L. Brown, H. C. Crookham, and R. L. Belford, FUEL, (in press) 1990.

"A SAW Oscillator-Based Modulator/Mixer for Frequency Modulated ENDOR," R. B. Clarkson, R. L. Belford, and C. Reiner, Rev. Sci. Instrum., (in press) 1990.

"EPR and ENDOR Studies of Perylene Radicals Adsorbed on Alumina and Silica-Alumina Powders", K. S. Rothenberger, H. C. Crookham, P. A. Snetsinger, R. B. Clarkson, and R. L. Belford, Abstracts of 10th International ESR Symposium, Denver, 1987.

"Electron Spin Echo Envelope Modulation Studies of Natural Abundance Low-Gamma Nuclei", P. A. Snetsinger, J. B. Cornelius, R. B. Clarkson, and R. L. Belford, 10th International ESR Symposium, Denver, 1987.

"Electron Spin Mapping of Coal Molecular Structure by ENDOR", R. L. Belford and R. B. Clarkson, invited paper, U. S. DOE Conference on University Coal Research, Pittsburgh, 1987.

"Enhancement of the Nuclear Modulation in the Electron Spin Echo Envelope at Low Magnetic Fields," H. C. Crookham, David R. Brown, Mark D. Timken, R. B. Clarkson, and R. L. Belford. 11th International EPR Symposium, Denver, August, 1988.

"ENDOR Spectra of Polycyclic Aromatic Hydrocarbon Cation Radicals and the Optimization of their Spectral Parameters by the Simplex Method," Karen J. Mattson, R. B. Clarkson, and R. L. Belford. 11th International EPR Symposium, Denver, August, 1988.

"A Novel S-Band Electron Spin Echo Spectrometer," David R. Brown, Harry C. Crookham, Mark D. Timken, R. B. Clarkson, and R. L. Belford. 11th International EPR Symposium, Denver, August, 1988.

"EPR and ENDOR Studies of Aromatic Sulfur Heterocycles on Catalyst Surfaces," R. B. Clarkson, R. L. Belford, Dennis J. Youn, and Harry C. Crookham. 11th International EPR Symposium, Denver, August, 1988.

"Spin-Mapping of Coal Structures with ESE and ENDOR", R. B. Clarkson and R. L. Belford, U.S. DOE University Coal Research Symposium, Pittsburgh, July, 1989.

"Magnetic and Molecular Structure in Coal", R. B. Clarkson, R. L. Belford, D. R. Brown, H. C. Crookham, K. J. Mattson, M. J. Nilges, Wei Wang, and D. J. Youn, invited keynote paper, 12th International Symposium on EPR, Denver, August, 1989.

"Structural Information from Multifrequency ESEEM", H. C. Crookham, D. R. Brown, R. B. Clarkson, and R. L. Belford, 12th International Symposium on EPR, Denver, August, 1989.

"ENDOR Spectra of Aromatic Radical Ions in Disordered Solids: Spectra and Analysis", D. J. Youn, K. J. Mattson, R. L. Belford, and R. B. Clarkson, 12th International Symposium on EPR, Denver, August, 1989.

"High-Field EPR: W-Band (95 GHz) Spectroscopy", M. J. Nilges, M. D. Timken, W. Wang, R. B. Clarkson, P. H. Davis, J. Forrer, and R. L. Belford, 12th International Symposium on EPR, Denver, August, 1989.

"Multifrequency Standards for EPR," R. L. Belford, invited lecture, Conference on Standards in EPR Spectroscopy, National Institute for Standards and Technology (NIST), Gaithersburg, 1989.

"Electron Magnetic Resonance Studies of Argonne Sample Bank Coals", D. L. Brown, H. C. Crookham, R. L. Belford, and R. B. Clarkson, invited paper, International Chemical Congress of Pacific Basin Societies, Honolulu, December, 1989.

"Multi-Dimensional EMR Studies of Coal", R. B. Clarkson, invited lecture, NMR Symposium, Rocky Mountain Conference on Analytical Spectroscopy, Denver, August, 1990.

"I. Determination of Quadrupole Couplings via L-Band, $B_0 \| B_1$ EPR. II. Surface Interactions of Perylene Adsorbed on Oxide Powders," K. S. Rothenberger, PhD Thesis, University of Illinois, Urbana (1989).

"Spin Echo and Millimeter Wave Studies of Disordered Solids," J. B. Cornelius, PhD Thesis, University of Illinois, Urbana (1987)

"X-Band ENDOR and S-Band ESEEM of Paramagnetic Disordered Solids," H. C. Crookham, PhD Thesis, University of Illinois, Urbana (1990).

"Computer-Assisted Analysis of EMR Spectra and ENDOR of Isolated Perylene Cations," K. J. Mattson, PhD Thesis, University of Illinois, Urbana (1990).

"S-Band ESE and Multifrequency EPR Studies of Some Disordered Solids," D. R. Brown, PhD Thesis, University of Illinois, Urbana (1990).

DISCLAIMER

END

DATE
FILMED
2/07/92